NASA TECHNICAL NOTE

NASA TN D-7755

NASA TN D-7755

COMPARATIVE EVALUATION OF PREDICTED AND MEASURED PERFORMANCE OF A 68-CUBIC METER TRUNCATED REVERBERANT NOISE CHAMBER

H. D. Cyphers, A. N. Munson, and F. J. On

Goddard Space Flight Center
Greenbelt, Md. 20771

NATIONAL AERONAUTICS AND SPACE ADMINISTRATION • WASHINGTON, D. C. • JANUARY 1975

1. Report No.	2. Government Accession No.	3. Recipient's Catalog No.
NASA TN D-7755		

4. Title and Subtitle	5. Report Date
Comparative Evaluation of Predicted and Measured Performance of a 68-cubic Meter Truncated Reverberant Noise Chamber	January 1975
	6. Performing Organization Code: 321
7. Author(s): H. D. Cyphers, A. N. Munson, and F. J. On	8. Performing Organization Report No.: G-7434
9. Performing Organization Name and Address: Goddard Space Flight Center, Greenbelt, Maryland 20771	10. Work Unit No.: 502-22-11-01
	11. Contract or Grant No.
	13. Type of Report and Period Covered: Technical Note
12. Sponsoring Agency Name and Address: National Aeronautics and Space Administration, Washington, D. C. 20546	14. Sponsoring Agency Code

15. Supplementary Notes

16. Abstract

The performance of a medium size, truncated reverberation chamber is evaluated in detail. Chamber performance parameters are predicted, using classical acoustic theory, and are compared to results from actual chamber measurements. Discrepancies are discussed in relation to several available empirical corrections developed by other researchers. Of more practical interest is the confirmation of a recent theory stating that the present guide for the ratio of specimen volume to test chamber volume, approximately 10 percent, is overly conservative, and can be increased by a factor of at least 2 and possibly 3. Results and theoretical justification of these findings are presented.

17. Key Words (Selected by Author(s))	18. Distribution Statement
Facilities, research, and support; Environmental test facility; Acoustic testing; Sonic testing; Reverberation chamber	Unclassified—Unlimited Cat. 14

19. Security Classif. (of this report)	20. Security Classif. (of this page)	21. No. of Pages	22. Price*
Unclassified	Unclassified	46	$3.75

*For sale by the Clearinghouse for Federal Scientific and Technical Information, Springfield, Virginia 22151.

This document makes use of international metric units according to the Systeme International d'Unites (SI). In certain cases, utility requires the retention of other systems of units in addition to the SI units. The conventional units stated in parentheses following the computed SI equivalents are the basis of the measurements and calculations reported.

CONTENTS

COMPARATIVE EVALUATION OF PREDICTED AND MEASURED PERFORMANCE OF A 68-CUBIC METER TRUNCATED REVERBERANT NOISE CHAMBER

H. D. Cyphers, A. N. Munson, and F. J. On
Goddard Space Flight Center

SUMMARY

The characteristics of the acoustic noise field produced within a 68-cubic-meter (2,400-cubic foot) truncated acoustic reverberation chamber were studied at Goddard Space Flight Center, and chamber performance results based on experimental data were compared to results predicted for a rectangular chamber of the same volume having theoretically optimum linear dimensions. Experimental data were also compared to results obtained from model studies.

For practical purposes, the acoustic noise field within the chamber is considered to be identical to the field predicted for the ideal chamber. The chamber thus meets the requirements for acoustic testing of small spacecraft systems and subsystems. Test specimen volumes of up to 20 percent of the chamber volume are shown to have a negligible effect on the acoustic noise field when measured on an averaged one-third-octave basis. Included in this paper is a detailed discussion of a means for determining the lowest usable frequency based on the structural excitation required and the minimum diffuse field which can be tolerated. As an aid in predicting the chamber's capability to meet any proposed type of performance specification, a series of curves is presented that show the limits of spectrum shaping available.

INTRODUCTION

The new reverberation chamber was constructed by the Structural Dynamics Branch at Goddard Space Flight Center to provide a means of experimentally verifying the results of theoretical studies in the areas of noise-field prediction and to determine the effects of various-sized test specimen volumes on the acoustic field. The chamber has also been used frequently to test small scientific spacecraft and experiments. These tests have resulted in an evaluation of the acoustic field produced within this new chamber when empty and with various test volume sizes.

At the time of completion of the empty chamber evaluation and before the series of tests using various test volume sizes began, the German Helios spacecraft required acoustical testing. This spacecraft, with an enclosed volume of approximately 14 cubic meters or

20 percent of the chamber volume, provided an opportunity to obtain data on the effects of exceeding the usual 10 percent ratio for test to chamber volume. This ratio has usually been considered the point above which a test volume begins to influence the chamber noise field. The results of this test are discussed in relation to the performance of the empty chamber.

There are two important performance characteristics used to specify a reverberation chamber's capability. These characteristics are the lowest usable test frequency and the ability to match the required spectra shapes and levels of launch vehicle specifications. Usable implies that the sound pressure level is reasonably uniform and that there are a sufficient number of modes within the fractional octave bandwidth to insure the proper excitation of the test article. To evaluate these characteristics, the following properties of the reverberation room were determined:

- Reverberation time (or effective absorption),
- Modal density (or modal overlap), and
- Spatial variation of the sound-pressure field.

Each of these areas is discussed in detail in the Test Results and Discussion section of this document.

DESCRIPTION OF TEST FACILITY

Room

Figure 1 is an isometric view of the reverberation noise test facility, which is a poured concrete chamber with an epoxy-painted interior. As mentioned above, the interior volume of the reverberant room is approximately 68 m^3 with a total surface area of 102.1 m^2 (1,100 $feet^2$). The maximum orthogonal dimensions are 5.27 by 4.18 by 3.34 m (17.3 by 13.7 by 11 feet), in the ratio 1.00:0.79:0.63, which has been suggested by Sepmeyer (reference 1) for good chamber performance. The floor plan is basically rectangular, with two adjacent walls bisected vertically to form a fifth wall. The entrance to the reverberant chamber is a steel door 2.74 m high by 2.13 m wide (9.0 by 7.0 feet). The practicability of this design was verified by a series of model studies conducted at Bolt, Beranek and Newman, Inc., as reported in reference 2.

The chamber, door, horn, and exhaust/silencer system have been designed for an overall noise reduction of 50 decibels to the outside of the chamber, provided that the cable and plumbing penetrations are properly sealed. All decibel notations are referenced to 20 X 10^{-6} N/m^2 unless otherwise noted.

The north and south interior walls and the floor and ceiling have been provided with a matrix of anchor points, measuring 2.54 by 2.54 m (100 by 100 inches), for convenience in locating microphones and for suspending test articles. The floor contains a 5,436-kilogram (12,000-pound) seismic block, which is centered on a point midway between the physical

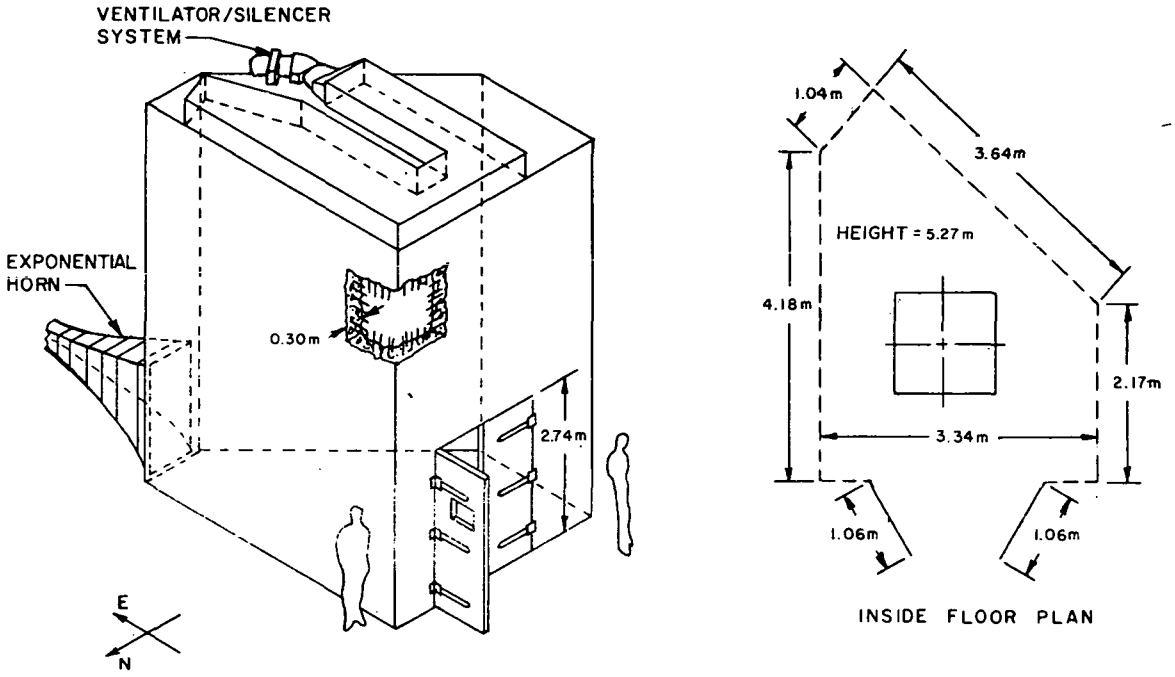

Figure 1. Goddard Acoustic Reverberation Test Facility

and geometrical centers of the floor plan. This block, 1.22 by 1.22 m (4 by 4 feet) is topped by a steel plate 5.08 cm (2.0 inches) thick, preloaded to 13.78 X 10^7 N/m^2 (20,000 psi). The block is accurately leveled and is tapped to match the MB-C210 vibration system mounting hole pattern.

Horn

The acoustic excitation is supplied to the reverberant chamber by an exponential horn which can be driven by either a Noraircoustic Mark V or a Ling EPT-94B air-modulator acoustic driver. As shown in figure 1, the exponential horn is coupled to the chamber through an opening 1.04 by 1.42 m (3.4 by 4.7 feet) at one end of the chamber.

The exponential horn consists of a fiberglass and steel liner encased in 25 cm (10 inches) of steel reinforced concrete. The horn has an overall length (including the extension through the chamber wall) of 3.02 m (119 inches) and a flare coefficient of 0.02. The cutoff frequency of the horn is estimated to be 60 Hz.

Driver

The two acoustic generators used to drive the exponential horn are remotely programmable types. The input-output specifications for these generators are shown in table 1.

The Noraircoustic Mark V generator consists basically of an electro-hydraulically driven poppet valve which provides 100-percent modulation of the high pressure airstream. It can respond to many types of electrical inputs, such as single impulses, periodic and complex waveforms, and wideband random noise.

Table 1

Input-output Specifications for Noraircoustic Mark V and Ling EPT-94B Noise Generators

Data	Noraircoustic Mark V	Ling EPT-94B
Output Acoustic Power	50 kW	4 kW
Air Supply Pressure	827.36 $N/m^2 \times 10^3$ (120 psig)	275.78 $N/m^2 \times 10^3$ (40 psig)
	1,241.04 $N/m^2 \times 10^3$ (180 psig)	
Air Flow Capacity	26.90 m^3/minute (950 scfm) 32.0 m^3/minute (1,130 scfm)	12.75 m^3/minute (450 scfm)
Hydraulic Flow	22.70×10^{-3} m^3/min at 17.2 $\times 10^6$ N/m^2 (6 gpm at 2,500 psi)	
Electrical Power	100 volt-amps	90 volt-amps

Note: psig = pounds per square inch gage.
scfm = standard cubic feet per minute.

The Ling EPT-94B acoustic generator is controlled by an electro-dynamically operated sleeve valve, and is also capable of reproducing impulse, periodic, and random input signals. These noise sources have previously been evaluated and reported.

Control and Data Collection System

The control and data collection system (figure 2) consists of standard, commercial, laboratory-quality equipment. The control panel provides central control, overall signal attenuation prior to the power amplifiers, and a monitoring point for the hydraulic and pneumatic inputs. The sound-pressure-level meter is a digital voltmeter with associated electronics; the meter has a dynamic range of 80 dB (10,000:1). Developed by GSFC laboratory personnel this meter is used to provide a continuous display of the overall sound pressure level during an acoustic test. One-third octave-band spectrum shaping and octave-band analysis are performed in real time. A one-third octave-band analyzer will replace the present octave-band analyzer in the near future. Special equipment setups were used to determine the reverberation time and the chamber modal density.

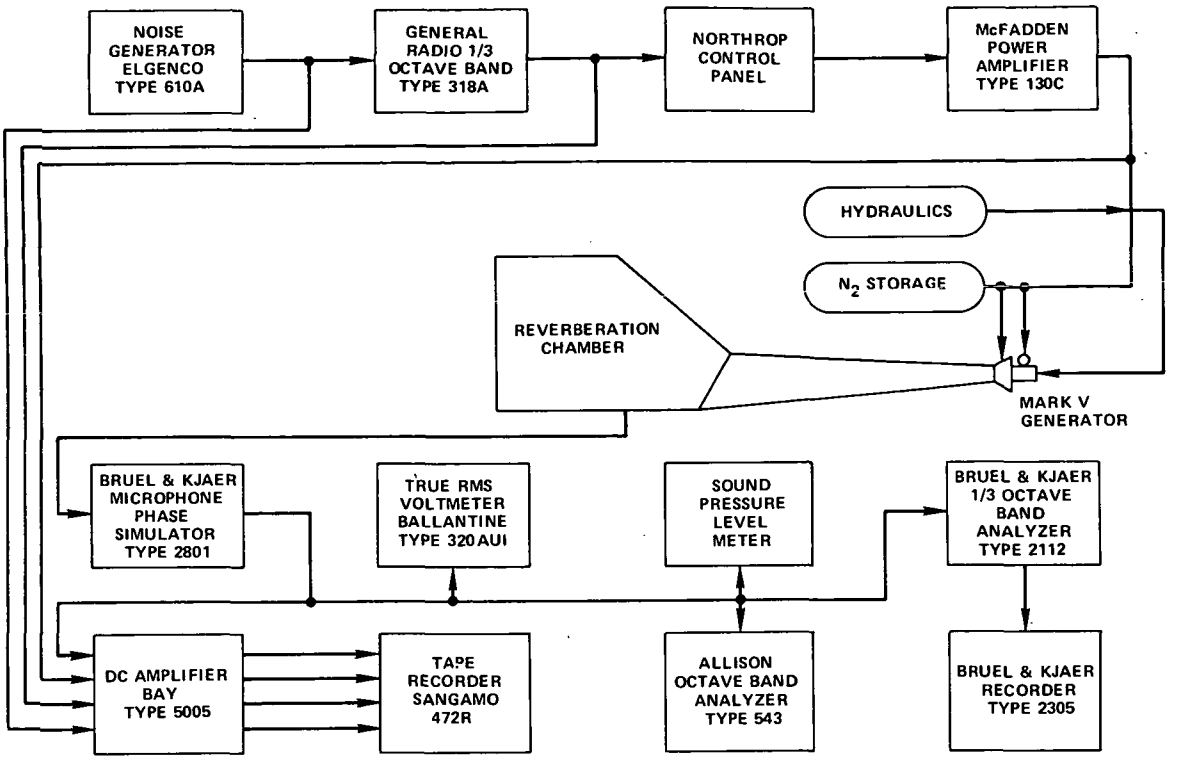

Figure 2. Equipment Setup for Random Noise Testing

TEST PLAN AND PROCEDURE

An overall test plan and a detailed test procedure were written for the evaluation of the reverberant noise chamber. Briefly summarized, the test plan and procedure specified tests to determine the chamber reverberation time, the sine sweep response and modal density, the spatial variation, and the spectrum-shaping capability of the generator-horn-chamber combination. The data from these tests were used to determine the characteristics of the reverberation chamber, including the lowest usable test frequency and the ability of the chamber to simulate the shapes and levels of launch vehicle noise spectra. These characteristics are the most important from the user's standpoint.

The characteristics of the acoustic sources operating into a progressive wave chamber 0.61 m^2 (2 $feet^2$) were determined in previous studies. These results in addition to the experience gained in operating the Noraircoustic Mark V generator into a large progressive-wave chamber of 79.25 m^3 (2,800 $feet^3$), the Launch Phase Simulator Acoustic System, provided sufficient knowledge of the effects of the generator input parameters on the generator output to determine the chamber performance.

Instrumentation and Data Analysis

The microphones were calibrated from sound pressure levels of 124 dB to 154 dB in 10-dB increments, using Bruel & Kjaer (B&K) Pistonphone and a Photocon Calibrator.

During the evaluation, both the frequency and amplitude response of the microphone and recording systems were checked periodically, because of the wide range of acoustic levels (114 to 170 dB) encountered. The microphone systems were checked for frequency response and voltage linearity by means of the voltage insert method. This procedure furnished a sound pressure level calibration to 154 dB and an insert voltage-linearity, voltage-frequency check to 180 dB, the upper limit of the microphone. The control and data collection system is identical to that used for the Noraircoustic Generator evaluation. Only the results for the control and recording system response to sine and random input signals will be summarized here.

Both the control and recording system are flat within ±0.5 dB from 30 Hz to 10 kHz. The power spectral density of the Mark V generator input, including noise source, one-third octave-band shaper, and power amplifier, is smooth and flat with no gaps over the frequency range 20 Hz to 2 kHz. The probability density plot of the generator output into a progressive wave chamber is gaussian with no skewness about the zero mean.

All off-line data analysis was done with the use of the power-spectral-density, one-third octave-band, and coherence algorithms of the Goddard dynamic data-analysis computer program (DYVAN). This program is designed to handle sinusoidal-sweep, shock transient, or stationary random data. The entire program contains more than 30 algorithms for converting input time histories into outputs, for example, probability distributions and spectral densities for tabular and graphic display on an on-line printer as well as in final hard-copy or microfilm plots.

Microphone Locations

In the experimental evaluation of the chamber properties, careful selection of microphone locations was required to measure accurately the acoustic field in the chamber. Because the sound-pressure levels in the chamber are higher nearer the walls, corners, and edges than throughout the rest of the room, all microphones were placed at least 3/4 λ away from the corners and edges of the chamber and at least $\lambda/4$ from the walls, where λ is the wavelength of the lowest frequency of interest.

To determine the reverberation time and room absorption, three microphones were located vertically along the center axis of the chamber at elevations of approximately 1.52, 3.04, and 4.12 m (5, 10, and 13.5 feet). For the modal density and modal overlap determination, the same three microphone locations were used.

When obtaining acoustic measurements for determining the spatial average and spatial variation; that is, the degree of spatial nonuniformity, of acoustic noise levels within the reverberant chamber, uncorrelated microphone outputs are desired. The greater the statistical independence (correlation approaching zero) between paired points, the higher is the degree of confidence that the spatial average and spatial variation data obtained are repeatable and are representative of the noise field at that point in space. Accordingly, the spatial separation between the paired locations was chosen to be large, when compared

with $\lambda/2$ or integral multiples of $\lambda/2$. This criteria was based on the fact that the theoretical point-to-point coherence ($C_{AB\Delta f}$) between the sound pressures in a reverberant sound field of narrow bandwidth Δf (see figures 3a and 3b) may be computed by the formula

$$C_{AB\Delta f} = \left[\frac{\sin\left(\frac{2\pi}{c} fr\right)}{\frac{2\pi}{c} fr} \right]^2, \qquad (1)$$

where r = distance in meters between the points at which pressure measurements are taken;

f = center frequency of the band in Hz; and

c = velocity of sound in meters/second.

The correlation coefficient is simply the square root of the coherence coefficient. Theoretically equation (1) is valid only under the conditions that the sound field is narrow band or discrete frequency, that it is undamped, that a high modal density exists with no two modes having the same frequency, and that all modes are excited to equal amplitude at one corner. In practice it is still reasonable to use this equation as a standard for approximating the uncorrelated separation distance between microphone measurement points, provided symmetry of points and excitations are avoided. The worst-case coherence results (computed by Goddard's DYVAN program), based on data from the reverberant chamber acoustic tests, have been presented in figures 3a and 3b. These figures indicate the approximate degree of statistical independence of the microphone outputs actually achieved via the use of the microphone locations. The results are discussed further in the section on Statistical Independence of Spatial Variation Data.

To keep the number of measurement points to a manageable level, the total number of microphones required for good statistical confidence may be minimized by optimizing the separation distance between microphones with respect to the wavelength of the frequency bands of interest. Figures 4a, 4b, and 5 show the microphone orientation in the chamber and the microphone array used for obtaining the spatial variation data in the empty chamber. For the empty chamber, four imaginary test-space cylinders with diameters of 1.68, 2.08, 2.52, and 2.68 m (66.0, 82.3, 99.2, and 105.6 inches) were generated as the microphone array was raised and lowered. In satisfying boundary conditions, the vertical height of the cylinders was limited to about 3.78 m (149 inches). The two smallest and two largest diameters represent the largest usable interior volumes while observing wall boundary restrictions for the two lowest frequencies of interest, 200 and 400 Hz, respectively. Accordingly, the sound pressure level measurements taken at the specified locations on the arrays and at the specified elevations (as the microphone array was raised and lowered) correspond to measurements taken at points on the surface of the four imaginary cylinders which meet the boundary restrictions and the requirement for relatively uncorrelated measurement outputs.

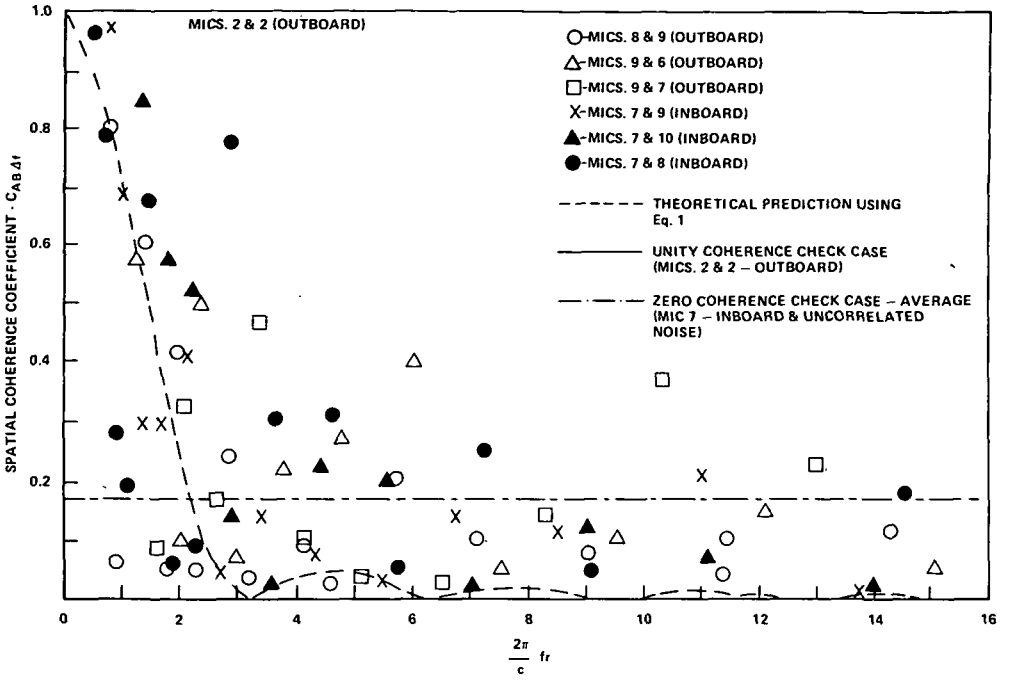

Figure 3a. Spatial Coherence Between Measured One-Third-Octave Sound Pressures Compared to Theoretical Coherence Between Narrow Band Diffuse Sound Pressures - Empty Chamber

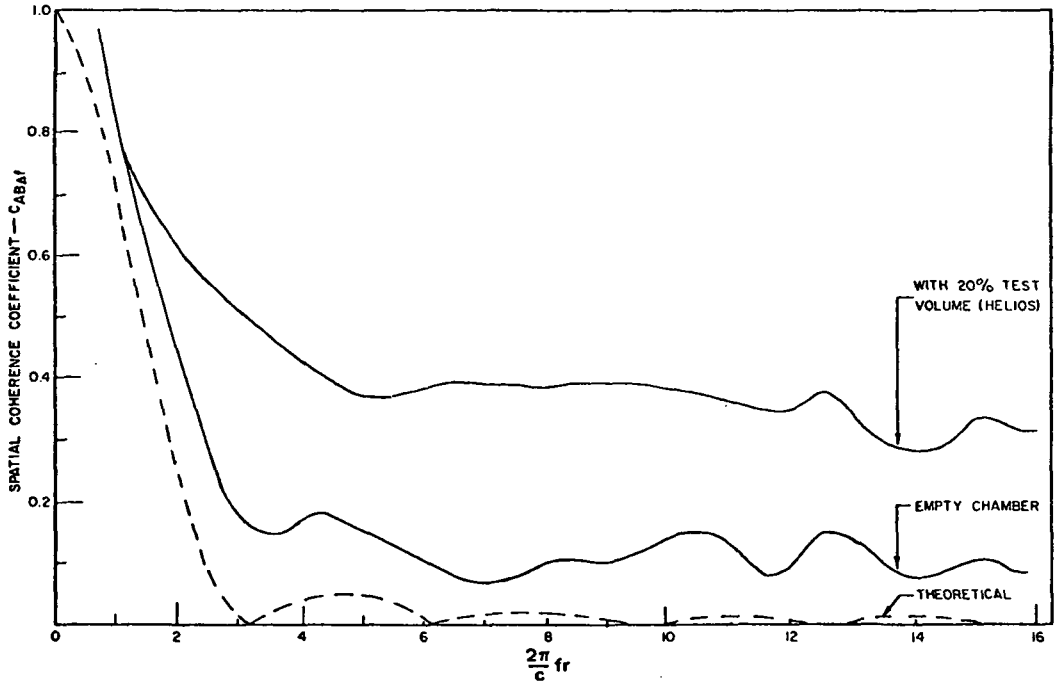

Figure 3b. A Comparison of Spatial Coherence for Both the Empty and Occupied Chamber (Based on Measured One-Third-Octave Sound Pressures)

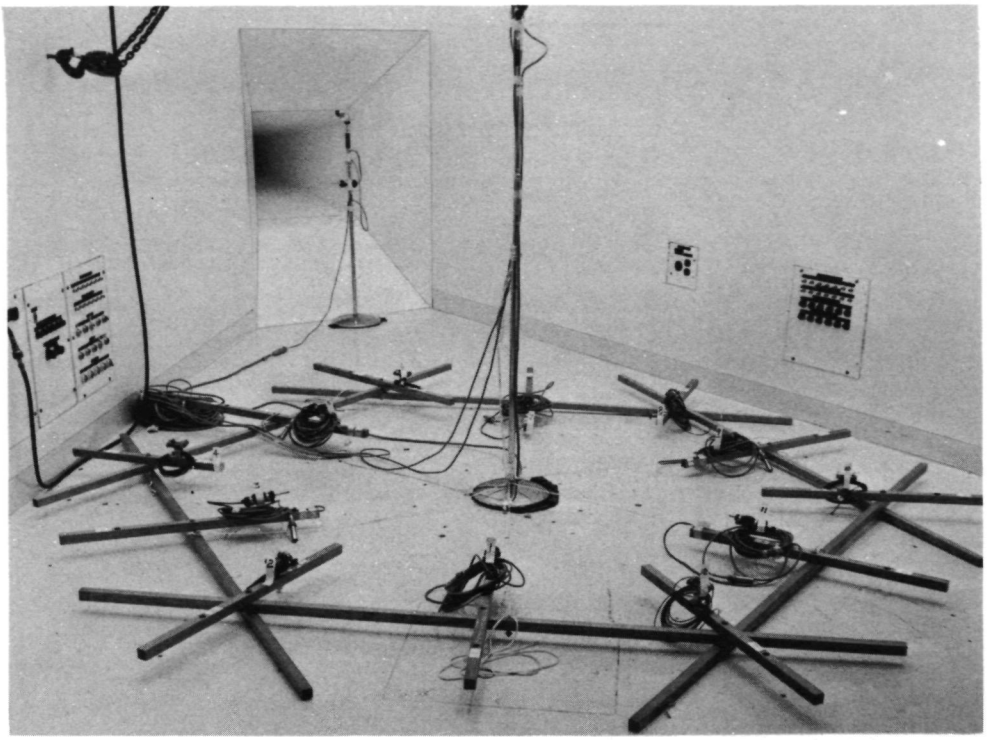

Figure 4a. Microphone Fixture Oriented in Chamber for Spatial Variation Tests - Empty Chamber

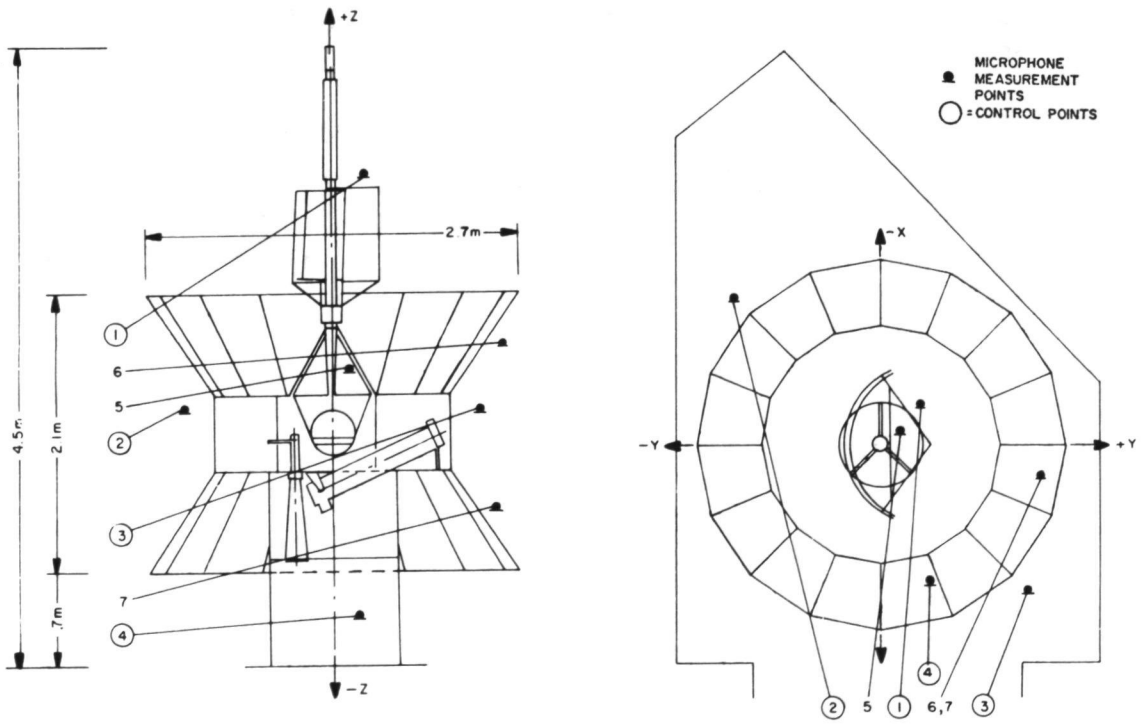

Figure 4b. Helios Spacecraft in Chamber Showing Microphone Locations

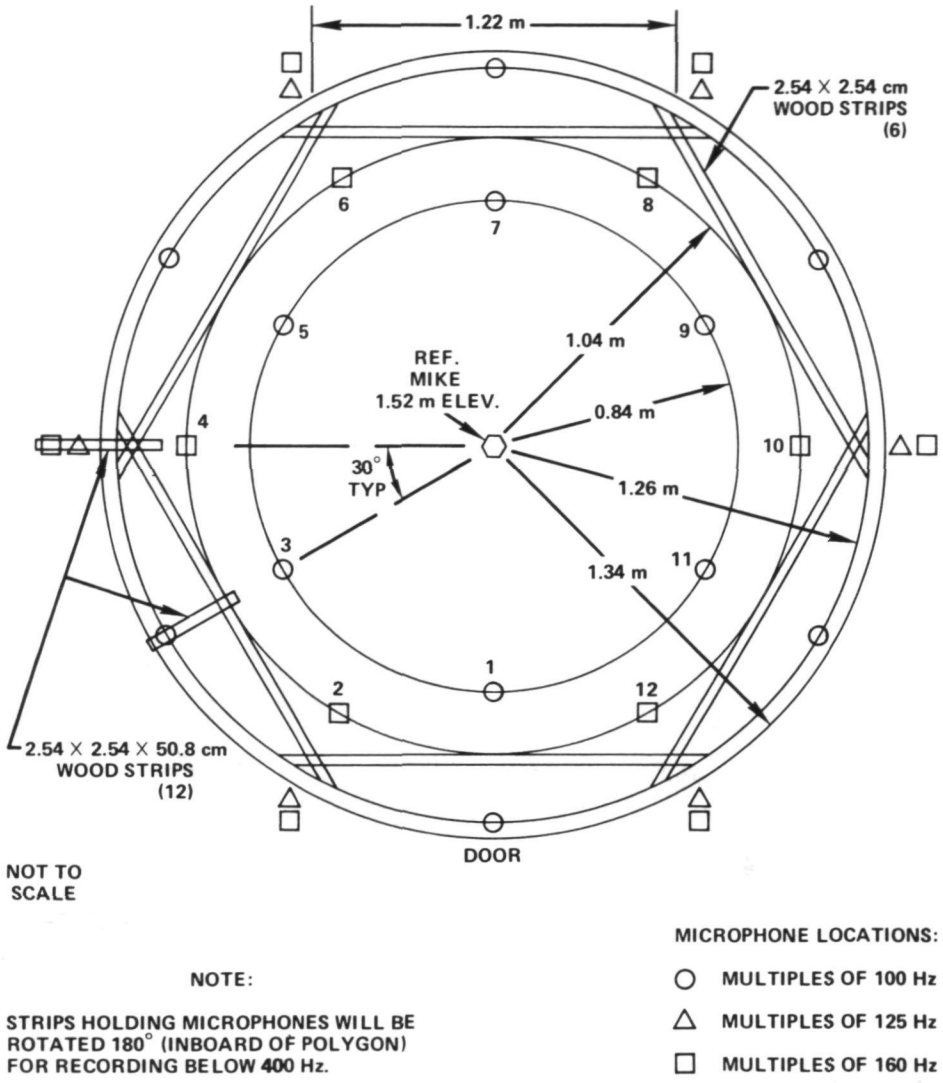

Figure 5. Plan View of Microphone Array and Fixture for Spatial Variation Tests

For the occupied chamber data, the microphone positions specified by the Helios test procedure were used (figure 4b); however, boundary conditions for the occupied chamber were not satisfied as they were in the empty chamber evaluation because of the size of the spacecraft.

TEST RESULTS AND DISCUSSION

The test results of the study can be categorized in terms of specific properties of the acoustic field within the reverberation chamber, and each property can be described from a theoretical standpoint. The predicted and measured results for the chamber, the method used

to obtain data, and the unusual features of the data are also described. The operational or performance characteristics of the reverberant acoustic facility, as derived from the measured properties, are summarized and discussed from theoretical and applicable points of view. The results of adding a 20-percent test specimen volume (Helios) will be discussed in relation to those tests. The necessity of obtaining chamber performance parameters during the actual Helios spacecraft test limited the ability to measure all of the desired properties. Data are presented for those properties that could be measured without interfering with the Helios test setup.

Reverberation Time (Effective Absorption)

The reverberation time for a given frequency is the time required for the average sound-pressure level, originally in a steady state, to decrease 60 dB after the source has ceased. This decay is caused by absorption of the sound energy not only at the boundaries of a room but in the air itself.

The reverberation time is related to the total effective absorption of the reverberant room by Sabine's equation (reference 3):

$$T_{60} = \frac{60V}{1.085c(a+4mV)} , \qquad (2)$$

where T_{60} = reverberation time in seconds

V = volume of room in cubic meters;

c = speed of sound in meters per second;

a = number of metric absorption units at the boundaries (walls) in square meters; and

m = energy attenuation constant in the transmitting medium in meters^{-1}

The term, a+4mV, is the total effective absorption.

The constant (m) is made up of two parts; one part arises from the effects of viscosity and heat conduction, and the other part from the effects of molecular (gas) absorption. The effects of viscosity and heat conduction are called classical absorption losses and are inherent in all gases due to basic gas transport phenomena. The principal effect of gas absorption involves an interaction of water vapor molecules with the resonance of oxygen molecules, so that the molecular absorption is highly dependent on the humidity content of the gas. The gas (molecular) absorption becomes significant at higher frequencies (above 1,000 Hz), and a knowledge of the absorption effects is necessary for predicting the attenuation in atmospheres other than air. This is of particular interest in this study, since the propagating medium used is gaseous nitrogen, which has a very low moisture content compared to air.

In practice the effective absorption is either obtained from tables that are readily available in the literature which list the absorption properties of various materials, or from a model study. In the chamber evaluated, the effective absorption losses were computed by utilizing model study data and a correction factor to account for the decrease in molecular absorption with the use of dry nitrogen.

Generally the reverberation time (T_{60}) and effective absorption (a+4mV) are plotted as a function of the center frequency of the fractional octave-band pressures. Figure 6 is a plot of the predicted and measured reverberation times. The times plotted are the average of three measurements taken at elevations 1.52, 3.04, and 4.12 m on a vertical line through the center of the chamber. Also plotted are the predicted and actual effective absorption coefficients. The actual effective absorption was calculated from equation (2). Table 2 is a tabulation of the reverberation times and the computed effective absorption at the three elevations. Figure 7 shows typical plots of reverberation time data at 80 and 400 Hz. For these measurements the chamber was excited with one-third octave-band random noise (approximately 114 dB, constant with frequency). Figure 8 shows the equipment setup used to obtain the measurements.

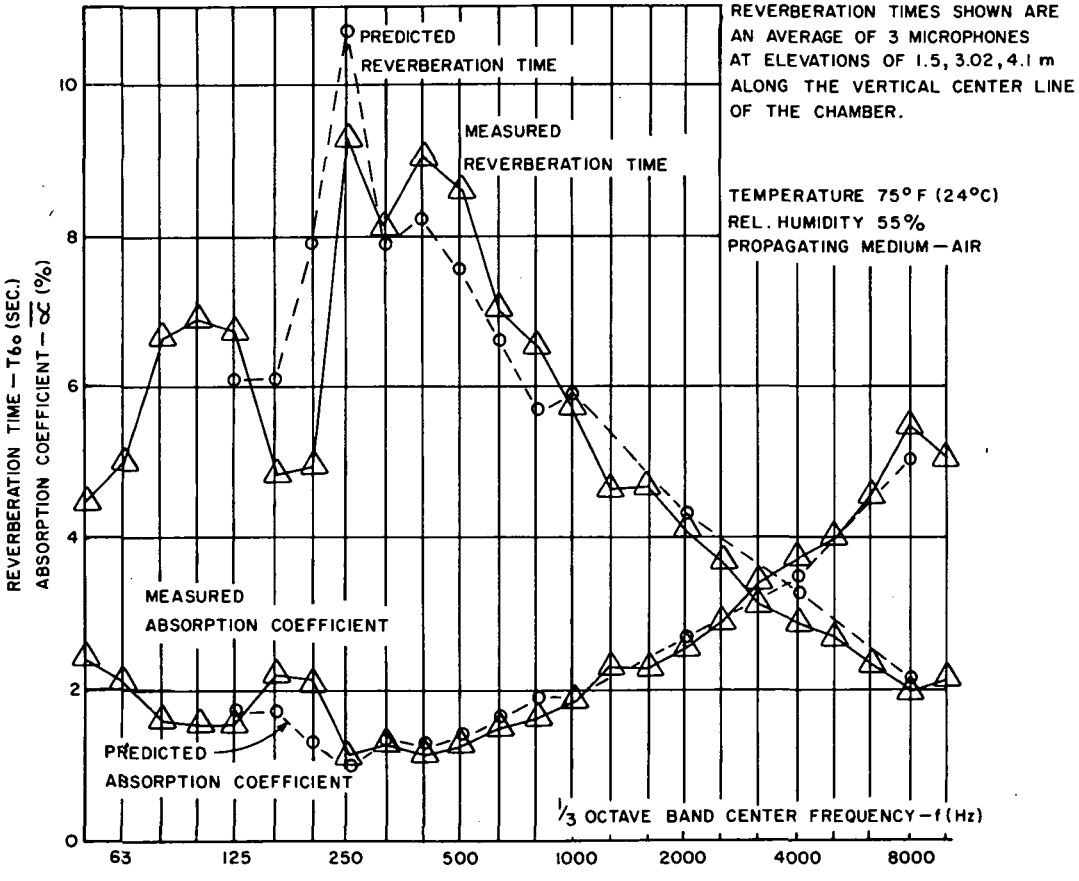

Figure 6. Predicted and Measured Reverberation Times and Absorption Coefficients - Empty Chamber

Table 2

Reverberation Times (One-third Octave-band Excitation)

One-Third Octave-Band	Reverberation Time (seconds)				Effective Absorption, $\bar{\alpha}$
	Microphones and Elevation			Average	$\bar{\alpha}=a+4mV=\frac{60V}{1.085cT_{60}}$
	1 (1.52 m)	2 (3.04 m)	3 (4.12 m)		
50 Hz	3.80[s]	6.0[s]	3.47[s]	4.42[s]	0.0241 m^2
	(9.6,11.0)*				
63	6.2	3.33	5.47	5.00	0.0213
	(16,10,7.47)	(20,11)	(17.67)		
80	5.80	7.73	6.33	6.62	0.0161
100	7.2	5.73	7.8	6.91	0.0154
125	7.4	6.8	6.13	6.78	0.0157
160	4.13	5.13	5.33	4.86	0.0219
	(7.13)				
200	4.10	4.6	6.2	4.97	0.0215
250	10.87	8.13	8.93	9.31	0.0114
315	7.8	7.73	8.87	8.13	0.0131
400	9.47	8.67	8.93	9.01	0.0118
500	8.8	9.0	8.07	8.62	0.0124
630	7.27	6.87	6.97	7.04	0.0151
800	6.8	6.4	6.53	6.58	0.0162
1,000	5.8	5.73	5.67	5.73	0.0186
1,250	4.6	4.67	4.73	4.67	0.0228
1,600	4.8	4.6	4.67	4.69	0.0227
2,000	4.13	4.07	4.27	4.16	0.0256
2,500	3.8	3.53	3.8	3.71	0.0288
	(5.1)	(4.7)	(3.27)		
3,150	3.4	2.93	3.07	3.13	0.0341
4,000	2.8	2.93	2.8	2.84	0.0376
5,000	2.47	2.93	2.6	2.67	0.0400
6,300	2.0	3.0	2.0	2.33	0.0458
8,000	2.07	1.87	1.93	1.96	0.0545
10,000	1.6	2.13	2.67	2.13	0.0501

* Values in parentheses not used in computing average reverberation time. These values are due to multiple slopes.

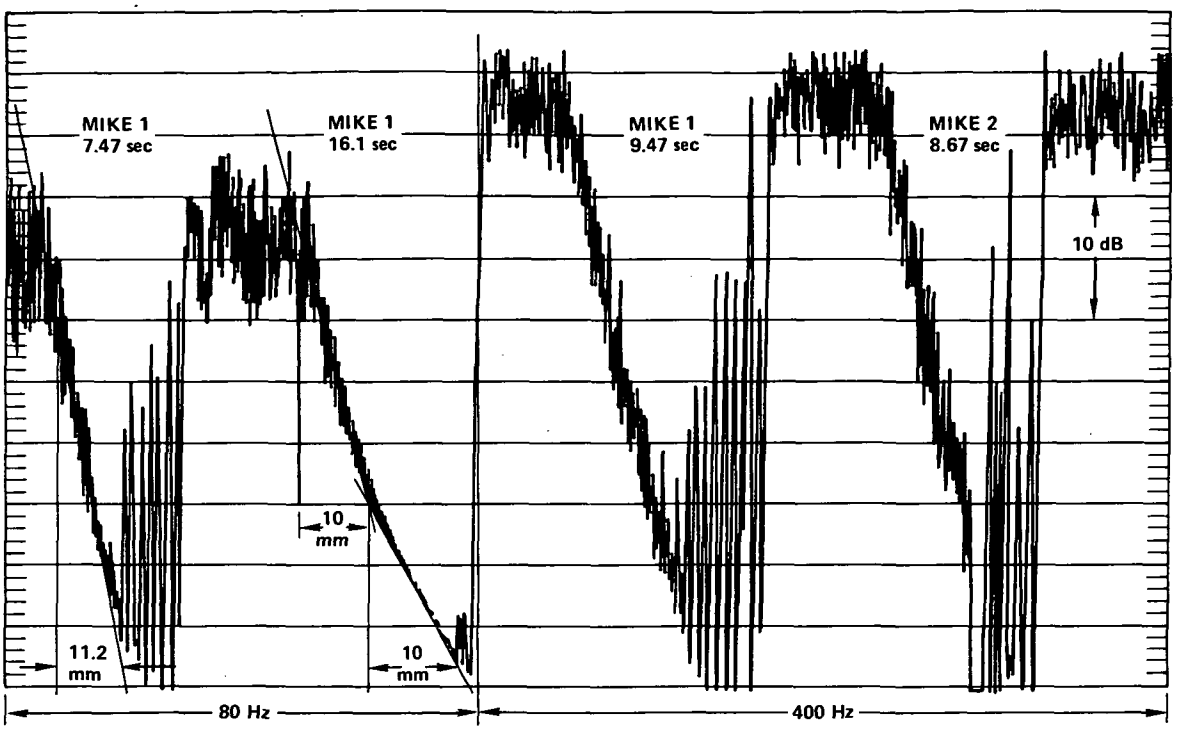

SAMPLE REVERBERATION TIME CALCULATION (80 Hz)
LEVEL HAS DECAYED 30 dB IN A DISTANCE OF 11.2 mm AT A PAPER SPEED OF 3 mm/sec.

$$T_{60\ dB} = \frac{2 \times 11.2\ mm}{3\ mm/sec} = 7.47\ sec$$

Figure 7. Reverberation Time Data (80 and 400 Hz)

The measured reverberation times possess some scatter, and are sometimes multivalued below approximately 400 Hz. Above 400 Hz the reverberation times decrease linearly with increasing log of frequency. The scatter at the lower frequencies is due to expected sound-pressure fluctuations in an enclosure of this size. This variation in sound-pressure level is one of the indicators used in determining the lowest usable frequency of the room. Morse and Ingard (reference 4) discuss in detail the reasons for the multiple slope and pressure fluctuation phenomena observed in some of the reverberation data (see table 2). Briefly, the explanation of the phenomena is as follows: When a sound source with a spread of frequency is used to excite a number of standing waves at the same time, the decay of these waves after the source is shut off is a rather complicated phenomenon. Spread as used here means containing frequencies other than a fundamental, in this case, one-third octave-band random noise. When only two or three standing waves have been excited and are decaying, they may alternately reinforce or cancel each other, because they are of slightly different frequency. The intensity then fluctuates with time instead of decreasing uniformly; the nature of the fluctuations depends on the position of the source and of the microphone in the room and on the manner of initiating the sound.

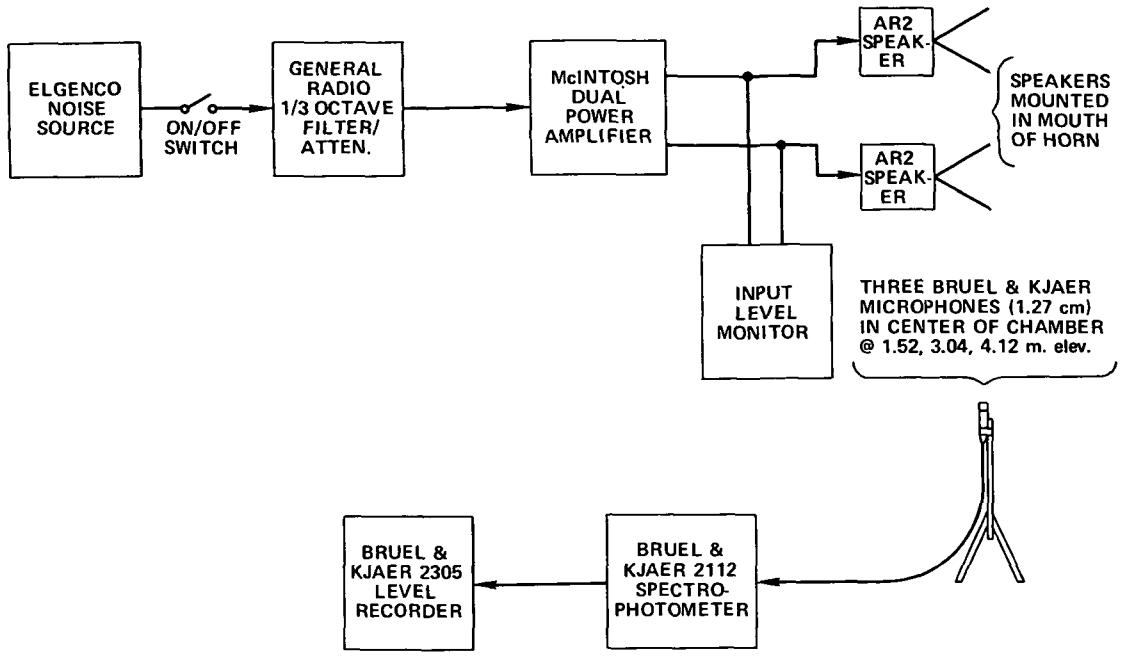

Figure 8. Equipment Setup for One-third Octave-band Reverberation Time Measurements

When more than three standing waves have been excited, the fluctuations will be more or less averaged out, and the resulting intensity will first diminish uniformly at a rate dependent on the reverberation time of the standing waves which are reflected from all six walls. After these oblique waves have decayed, the remaining sound, which is due to waves tangential and axial not striking all the walls, remains and dies out more slowly. The intensity level as a function of time approximates a broken line: the steeper, initial part corresponds to the decay of most of the standing waves, and the less steep part to the decay of waves that do not strike some of the walls. In such cases, the term reverberation time has a specific meaning only in connection with the damping out of single, normal modes; that is, only in connection with the slopes of the two portions of the broken line of intensity level against time. The actual length of time that it takes for the intensity level to drop 60 dB will depend on the relative amounts of energy possessed by the rapidly-damped and the slowly-damped standing waves.

Several other means of exciting the chamber were tested to determine the effects of various types of excitation on the reverberation time. Figure 9 is a plot of reverberation times obtained by using wideband white noise and discrete frequency excitation. As expected, the discrete frequency excitation values differ significantly from random noise excitation, especially below 400 Hz, because fewer standing waves are excited at a given time. The wideband white noise excitation (with the microphone response filtered on a one-third octave basis) agrees quite closely with the previous data. Although other experimenters seem to prefer one-third octave-band excitations, it appears that wideband white noise excitation can provide representative data at considerably less effort and expense.

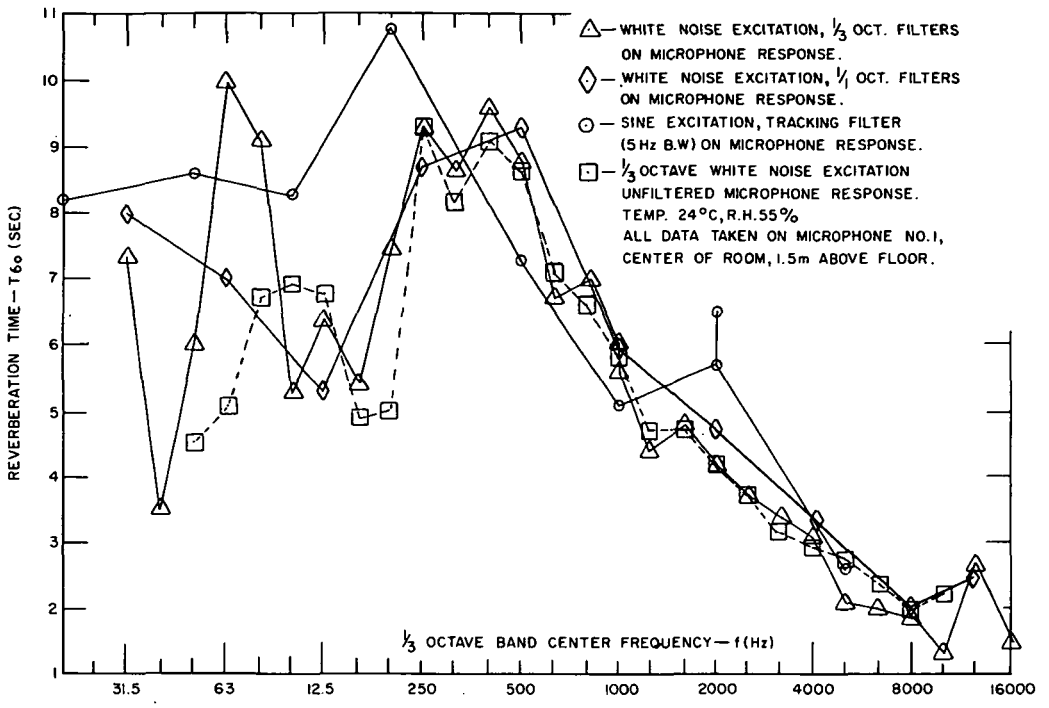

Figure 9. Reverberation Times Using Various Types of Excitation

In the scaled model study (reference 1), absorption coefficients were calculated from actual reverberation times for both the truncated and rectangular model chambers. The absorption coefficients for the two configurations were approximately the same at all frequencies. Since the data on predicted and measured reverberation times (figure 6) show that the calculated absorption coefficient for the Goddard chamber agrees with the predicted absorption using the model study results, it may be assumed that the reverberation times will bear the same relationship. That is, the reverberation time of the truncated chamber is approximately 85 percent of the reverberation time of an equivalent rectangular chamber (with dimensions equal to the parallel dimensions of the truncated chamber), in accordance with the dependency of the reverberation time on the volume-to-area ratio of the two chambers. No reverberation time data were obtained for the occupied chamber condition.

Modal Density, Sine Sweep Response, Modal Overlap

The frequency response of a reverberation room is characterized by a series of discrete resonant modes. For a simple, normal, rectangular room the lowest or first of these resonant modal frequencies occurs when one-half the acoustic wavelength equals the longest dimension of the room. The second resonant frequency occurs when one-half the wavelength equals the next longest dimension of the room. An entire harmonic series containing integer multiples of the fundamental axial modes exists for each of the three axes of the room.

At frequencies greater than those of the fundamental axial modes more complex modes appear. These include modes associated with four walls in which the standing waves are tangential to one pair of walls, and oblique modes that involve the interaction of standing waves between all six walls.

The aim in reverberation chamber design is to achieve a sound field within the volume which is completely diffuse in all frequency ranges of interest. This implies that there are many modes uniformly spaced in frequency, and that all angles of incidence of the sound are equally probable.

The modal frequencies of a rectangular chamber can be calculated from the characteristic equation given by (reference 5):

$$f_{m,n,p} = \frac{c}{2}\left[\left(\frac{m}{L_x}\right)^2 + \left(\frac{n}{L_y}\right)^2 + \left(\frac{p}{L_z}\right)^2\right]^{1/2}, \qquad (3)$$

where c = the speed of sound in air (meter/second);

L_x, L_y, L_z = the room dimensions in meters; and

m, n, p = mode numbers for the x, y, and z modes, respectively, and take on the integer values 0, 1, 2, 3, . . . etc.

When any two of the mode numbers are zero, the modes are purely axial (one-dimensional). When only one mode number is equal to zero, the modes are called tangential (two-dimensional), and when all three mode numbers are greater than zero, the modes are called oblique (three-dimensional). Near the fundamental frequency of the room, the mode number dependency of the effective absorption coefficient contributes to nonuniformity of sound level with frequency. As an approximation, equation (3) was used in estimating the modal frequencies of the Goddard truncated chamber. Table 3 compares predicted and measured chamber resonances. Only the modes which most nearly correspond to the predicted modes are tabulated. The actual data, shown in figures 10a, 10b, 10c, and 10d, indicate that many more modes are actually excited. Extensive computation of the modal frequencies of reverberation rooms using the classical equation (3) is tedious unless handled by computers. It is generally more significant to know the approximate number of acoustic modes that might be excited within any given bandwidth, that is, the product of modal density and bandwidth.

Modal Density [n(f)]

Modal density is the frequency distribution of the acoustic modes (the number of modes per unit frequency bandwidth) in the room due to the excitation of the room by a sound source. The modal density is dependent largely on the physical dimensions of the enclosure and the excitation frequency.

Table 3

Comparison of Calculated Modal Frequencies with Measured Modal Frequencies at Chamber Center*

Mode Numbers X:Y:Z	Calculated** Frequency (Hz)	Measured Frequency (Hz)
001	33.175	33.0
010	51.271	50.5
100	56.400	55.5
011	61.068	65.0
101	65.434	65.5
002	66.350	65.5
110	76.221	74.5
111	83.128	78.0
012	83.852	80.5
102	87.083	87.5
112	101.055	99.0, 100
020	102.544	103.0
021	107.777	108.0
200	112.800	112.0, 114.5
120	117.031	115.0
201	117.577	119.0
121	121.642	122.0
022	122.138	123.0
210	123.905	–
211	128.270	127.0

* Microphone at a height of 1.52 m.

** L_x = 3.04 m, L_y = 3.34 m, L_z = 5.27 m.

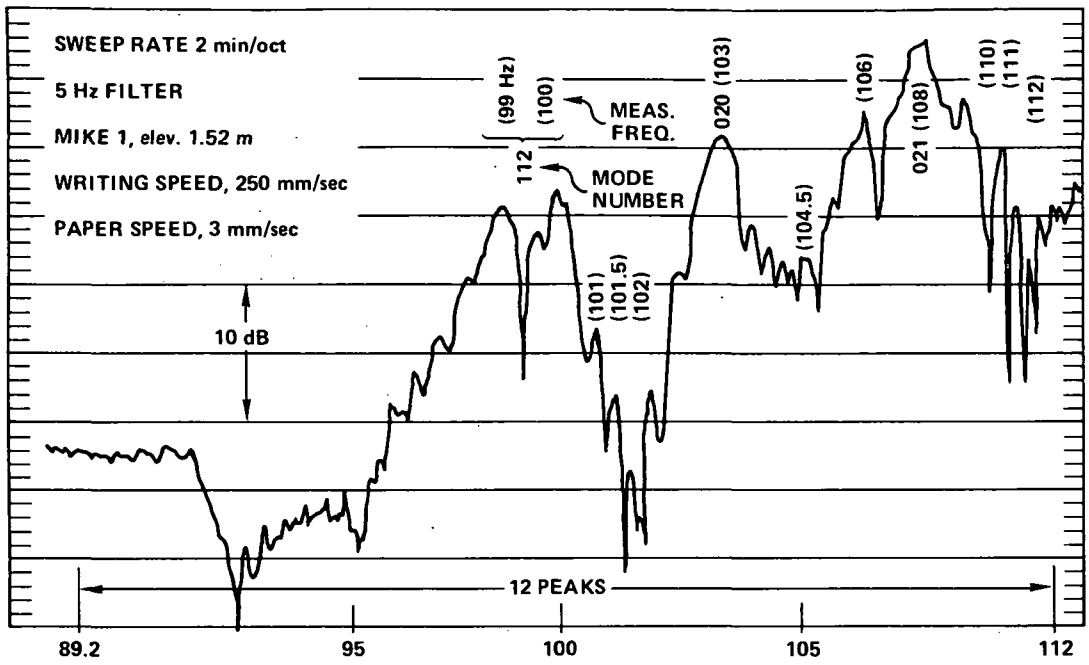

Figure 10a. Sine Sweep Response

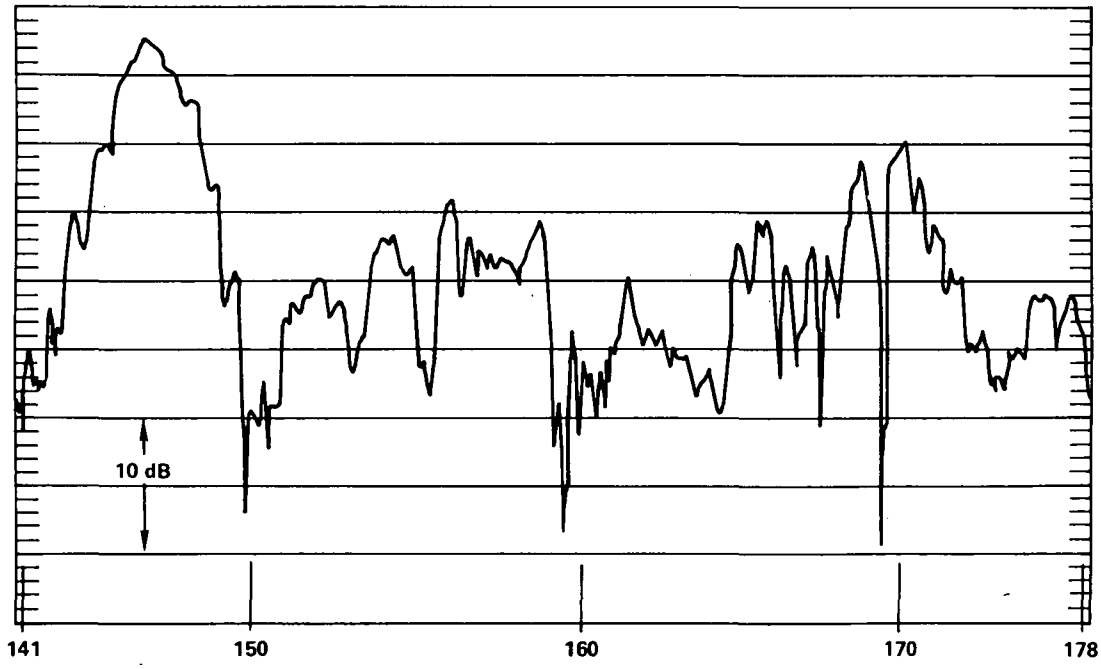

Figure 10b. Sine Sweep Response

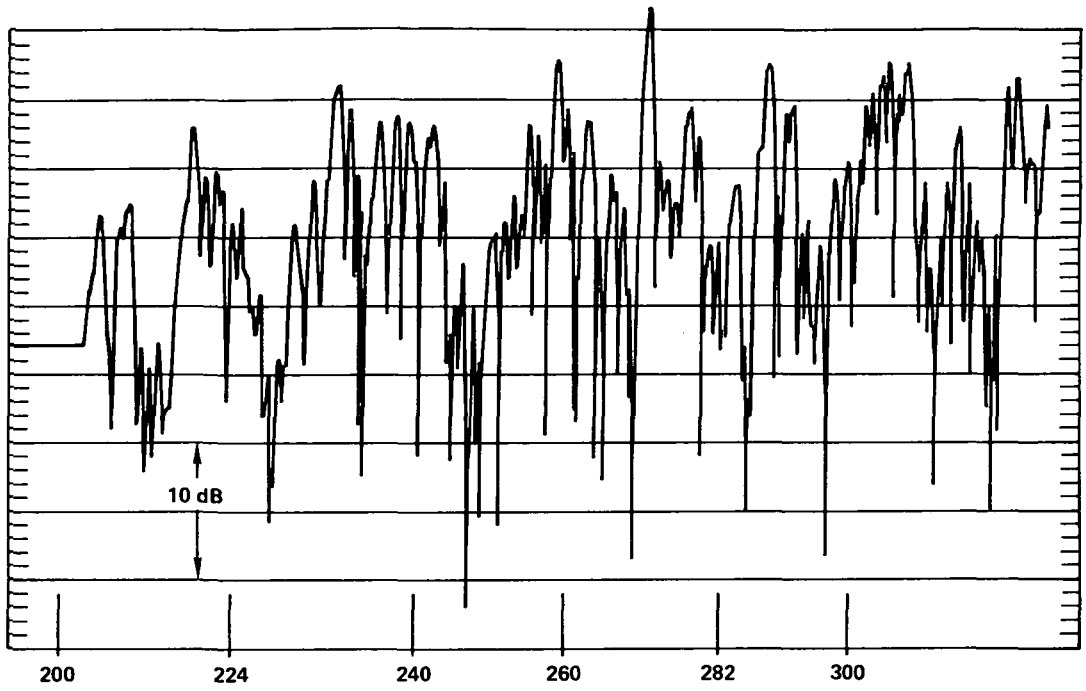

Figure 10c. Sine Sweep Response

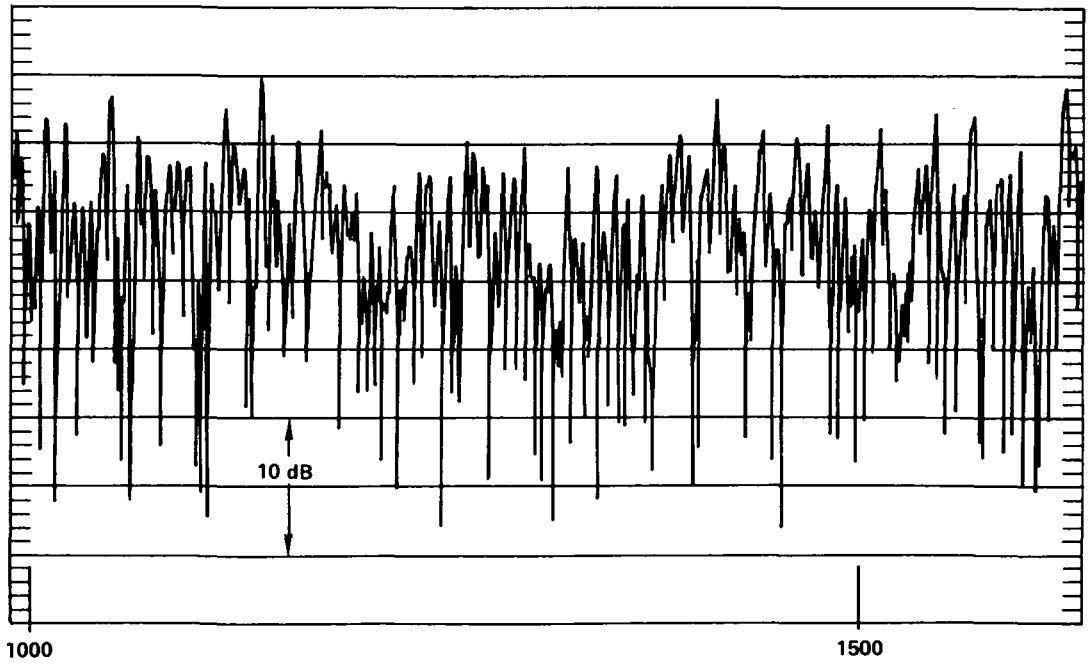

Figure 10d. Sine Sweep Response

The asymptotic modal density of a rectangular reverberation room may be computed by equation (4), which is derived from equation (3) (reference 6):

$$n(f) = \frac{4\pi f^2 V}{c^3} + \frac{\pi f A}{2c^2} + \frac{P}{8c} \quad , \tag{4}$$

where P = length of chamber wall intersections (total length of all chamber edges);

V = volume in cubic meters;

A = surface area in square meters;

c = velocity of sound; and

f = frequency.

This equation has also been shown to be applicable to this particular truncated chamber shape (reference 1). Accordingly, the number of resonant modes of the truncated chamber in each band of frequencies Δf may be computed by

$$N_{\Delta f}(f) = n(f)\,\Delta f = \left(\underbrace{\frac{4\pi f^2 V}{c^3}}_{\text{(Vol.)}} + \underbrace{\frac{\pi f A}{2c^2}}_{\text{(Surf.)}} + \frac{P}{8c} \right) \Delta f, \tag{5}$$

where f is center frequency of the band.

Alternatively, the cumulative resonance frequency distribution, that is, the integral of the modal density,

$$N(f) = \int_0^f n(f)\,df = \frac{4}{3}\,\frac{\pi f^3 V}{c^3} + \frac{\pi f^2 A}{4c^2} + \frac{Pf}{8c} \quad , \tag{6}$$

may be determined for comparison with a cumulative count of the sine sweep peaks, obtained by counting the number of modes excited during a sinusoidal sweep survey of the chamber.

Sine Sweep Response

The equipment setup shown in figure 11 was used to excite the room resonances. Three microphones were again located at the same elevations at the center of the chamber. When making the sine sweeps, the sweep rate and the direction of sweep, up or down, had a bearing on the number of resonances excited. A sweep rate of 2 minutes per octave gave good modal definition and repeatability when sweeping from either direction.

Figure 12 is a plot of the predicted modal density [n(f)], predicted cumulative resonance frequency distribution [N(f)], and the predicted and measured mode counts ($N_{\Delta f}$) for each one-third octave band in the chamber. Table 4 is a listing of the actual mode count

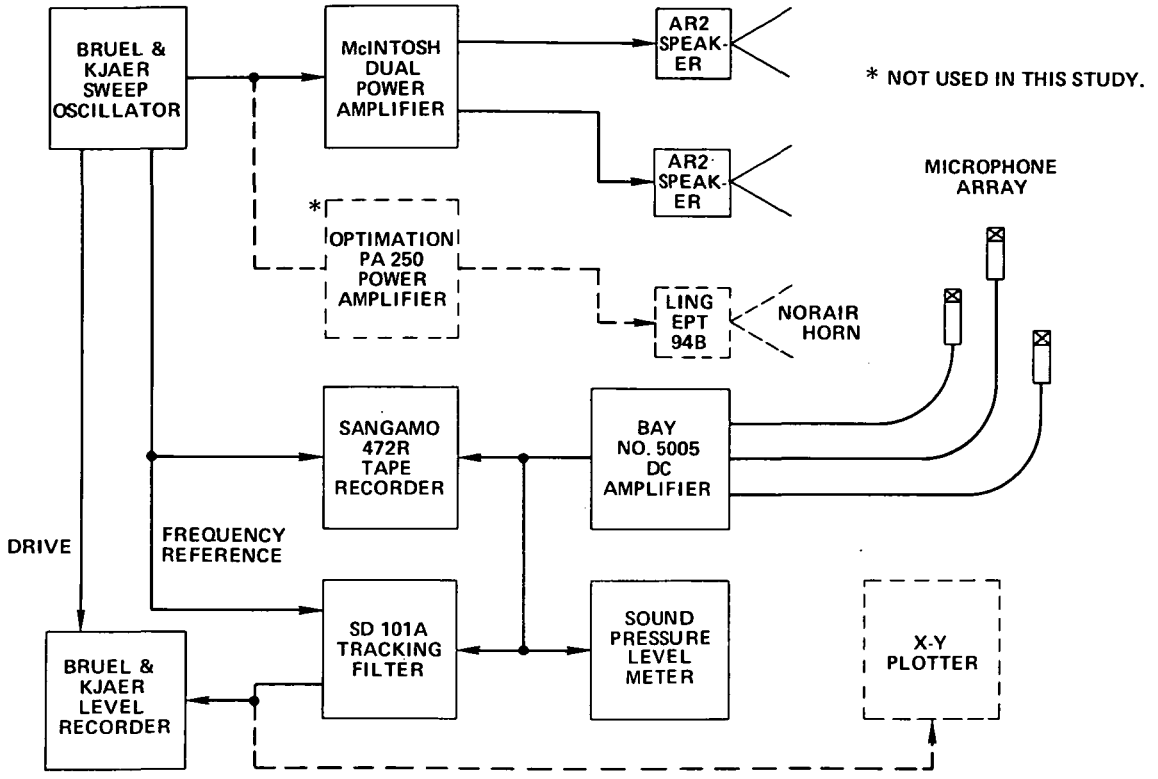

Figure 11. Equipment Setup for Determining Chamber Modal Density

versus that predicted using equation (5). Figures 10a, 10b, 10c, and 10d, typical plots of the chamber response data, illustrate the method used to count the room modes. The criterion used for counting the sine sweep response peaks required that the peak-to-valley ratio, on both sides of the peak, be 3 dB or more in order that the peak be counted.

For the chamber under study, the results presented in figure 12 and table 4 indicate that equation (5) provides a conservative prediction of the number of modes on a one-third octave-band basis. The results of figure 12 also indicate that above approximately 250 Hz the resonance peak count method greatly underestimates the number of modes that actually exist. This deviation from the predicted distribution is due to two causes: (1) some of the peaks are missed in the counting procedure when the response peaks are closely spaced in frequency; (2) many response modes occur within the bandwidth of a single mode. In these cases, counting the response peaks does not yield an accurate measure of the actual number of modal resonances (reference 7). The first cause can be minimized by using a higher paper speed to expand the frequency scale.

Also shown on figure 12 is the measured one-third octave-band mode counts of the occupied chamber. The number of modes is seen to be considerably lower than for the empty chamber condition. This is due primarily to the way the data were taken. The data were obtained by counting the peaks in a power spectral density plot of the microphone response, using a 2-Hz analysis bandwidth. The peak-to-valley mode height criterion

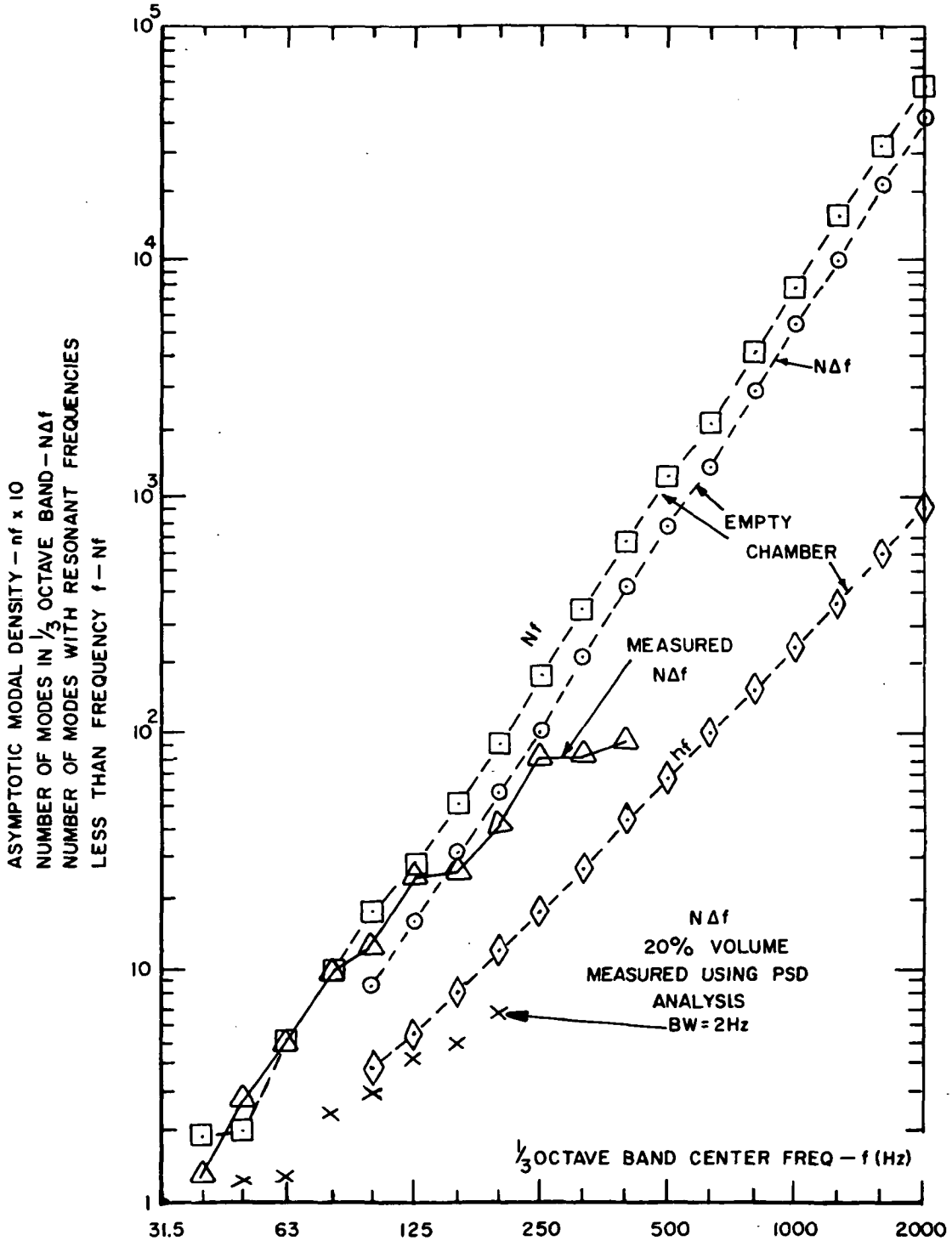

Figure 12. Predicted Modal Density n(f), Cumulative Resonance Frequency N(f), and Predicted and Measured Mode Counts ($N_{\Delta f}$)

Table 4

Comparison of Measured and Predicted Mode Count for
One-third Octave Bands - Empty Chamber

Frequency Hz		Measured Mode Count				Predicted $N_{\Delta f}$ (f) [Equation (5)]
Center	Upper & Lower Bandedge	Microphones 1	2	3	Average	
31.5	28.2 35.5	4	1	–	–	–
40	35.5 44.7	1	1	5	2	–
50	44.7 56.3	2	2	1	2	1.2
63	56.3 70.9	4	5	5	5	2.5
80	70.9 89.2	11	12	6	9.6	5
100	89.2 112.0	12	13	–	12	9
125	112.0 141.0	25	26	20	23.6	17
160	141.0 178.0	25	31	25	27	30
200	178.0 224.0	48	46	43	46	58
250	224.0 282.0	83,43	–	–	–	100
315	282.0 355.0	79,39	–	–	—	200
400	355.0 447.0	90	–	–	–	370
500	447.0 563.0	–	–	–	–	800

used during the empty chamber sine sweep evaluation was reduced to ±1 dB to account for the averaging effect over the 2-Hz bandwidth. Because of the relatively broad analysis bandwidth used, this method of counting modes is very conservative. Based on a criteria of a minimum of seven modes per one-third octave bandwidth, the chamber is usable (considering only the mode count) down to 80 Hz.

Modal Overlap (M)

The modal overlap index provides a measure of the diffuseness of the noise field in a well-designed reverberation room. It is defined as the number of adjacent modes which lie inside the 3-dB bandwidth of a typical chamber modal resonance. Computationally, it is the product of the 3-dB bandwidth $\Delta(f)$, and the average modal density, n(f):

$$M(f) = \Delta(f) \quad n(f) \tag{7}$$

where

$$\Delta(f) = 2.2/T_{60} .$$

The 3-dB bandwidth of a typical chamber modal resonance, $\Delta(f)$, is defined by the chamber resonant Q determined from the reverberation time. It will be recalled that one-third octave-band noise excitation was used in this study to establish reverberation times. The modal density, n(f), as shown in figure 12, is the average number of modes that exist at the center frequency of the one-third octave band of interest.

The product of the 3-dB bandwidth, $\Delta(f)$, and the average modal density, n(f), assumed constant over the bandwidth used when counting the modes, yields a figure of merit in terms of modes per chamber resonant bandwidth. This term and the spatial variation of sound pressure levels in the chamber provide a means of specifying the lowest usable frequency of the chamber. Selection of an appropriate value of M(f) is considered further in the section on selecting the lowest usable frequency. Figure 13 shows the predicted and measured values of modal overlap. Above 250 Hz it was necessary to use predicted values for the modal overlap due to the difficulty in measuring the modal density by the peak response count method. The modal overlap was not computed for the occupied chamber because of the lack of reverberation time data.

Spatial Variation (S)

The degree of spatial nonuniformity (commonly termed spatial variation) of acoustic noise levels in the reverberant acoustic chamber was determined in terms of the standard deviation, S, of sound pressure level. The deviation was computed from a sufficiently large set of uncorrelated sound pressure levels measured at specified locations in the chamber with a specific noise excitation. In figure 13 the predicted and measured results of spatial variation for the reverberant chamber are presented. The modal overlap has also been plotted in this figure to facilitate the application of the criteria for determining the lowest usable frequency of the chamber.

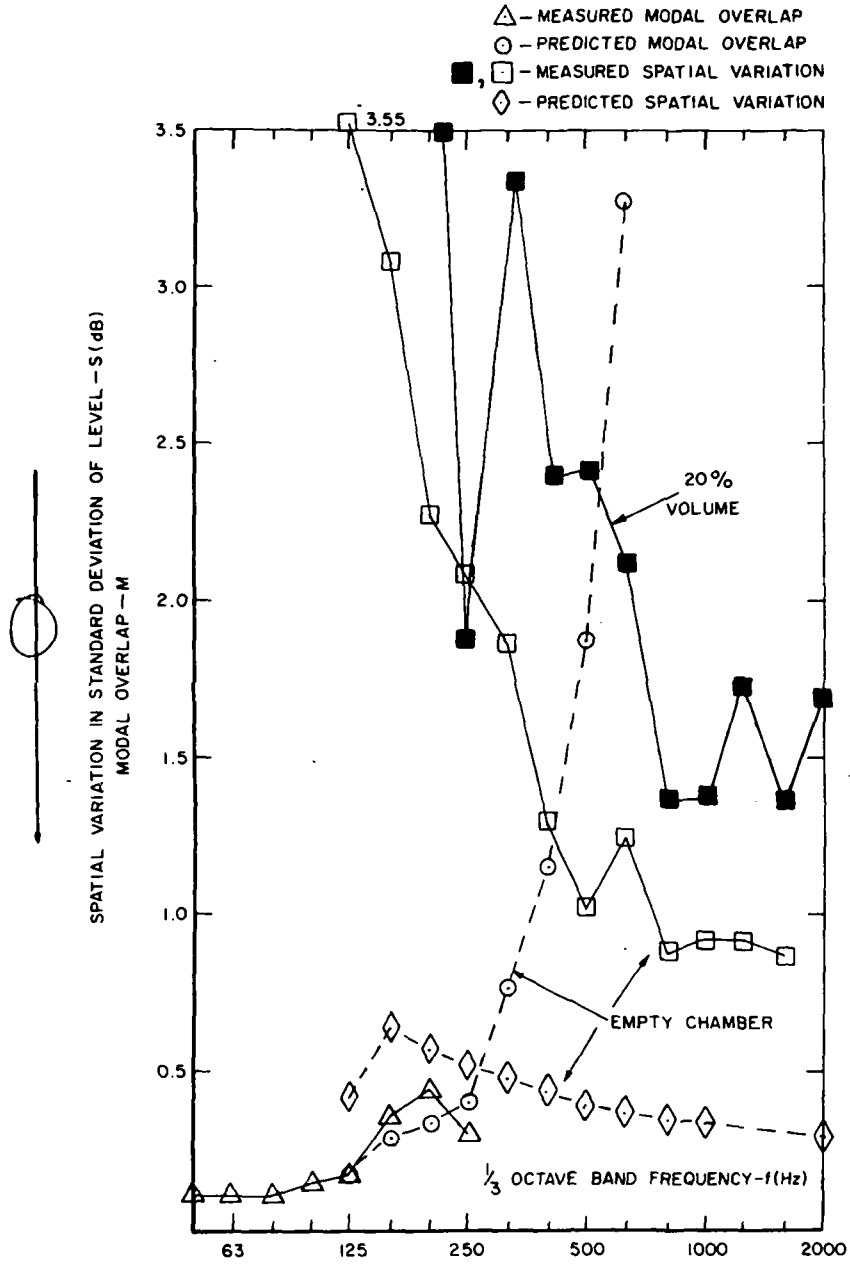

Figure 13. Predicted and Measured Modal Overlap and Spatial Variation - Empty Chamber and 20-percent Test Specimen Volume

The predicted results shown in figure 13 were obtained in the following manner: In the high frequency range (modal overlap >1) spatial variations were predicted by (reference 1):

$$S = 5.6\,(1 + 0.23\,BT_{60})^{-1/2}\ \text{dB} \tag{8}$$

where S, the standard deviation = the theoretical minimum for a perfectly diffuse field; and

B = the equivalent flat spectrum bandwidth of the excitation source. (For example, $B = 0.23\,f_0$ for one-third octave band, where f_0 is band center frequency.)

In the low frequency range, spatial variation predictions were based on the measured spatial variation of a truncated chamber model (reference 1), but scaled to the Goddard chamber on the basis of modal overlap index.

The measured, empty-chamber spatial variation results were determined from a set of 72 sound-pressure levels, L_i, measured at specified locations. In terms of standard deviation, S, the spatial variation was computed from

$$S = \left[\frac{n\sum_{i=1}^{n} L_i^2 - \left(\sum_{i=i}^{n} L_i\right)^2}{n(n-1)}\right]^{1/2} \tag{9}$$

where n = 72 is the total number of measurements in the set. This determination was repeated for each one-third octave band and is independent of the mean level; that is, S would not change if the experiments were repeated at a different sound-pressure level. S is also independent of time since the individual sample levels, L_i, were already time-averaged quantities computed via the DYVAN program.

As stated previously, the design of the array was dictated by boundary restrictions and by the requirement for uncorrelated measurements, and the test setups were shown in figures 4a, 4b, and 5. The 200-Hz measurements were taken with the microphones as shown in figure 4a; for the 400-Hz measurements the microphones were rotated outboard 180 degrees. To ensure a constant room excitation level (±0.6 dB) during the measurements, the acoustic-source overall level and spectral content were continuously monitored in real time via a fixed reference microphone as the microphone array was raised by remote control, starting at a height of 0.61 m in 0.76-m increments. In this manner, the array of microphone outputs was recorded independently for each elevation. Figures 14, 15, and 16 show a one-third octave-band analysis, a power spectral density (PSD), and a probability density analysis (PDA), respectively, of the reference microphone output (microphone 13), located at the center of the chamber at an elevation of 1.5 m.

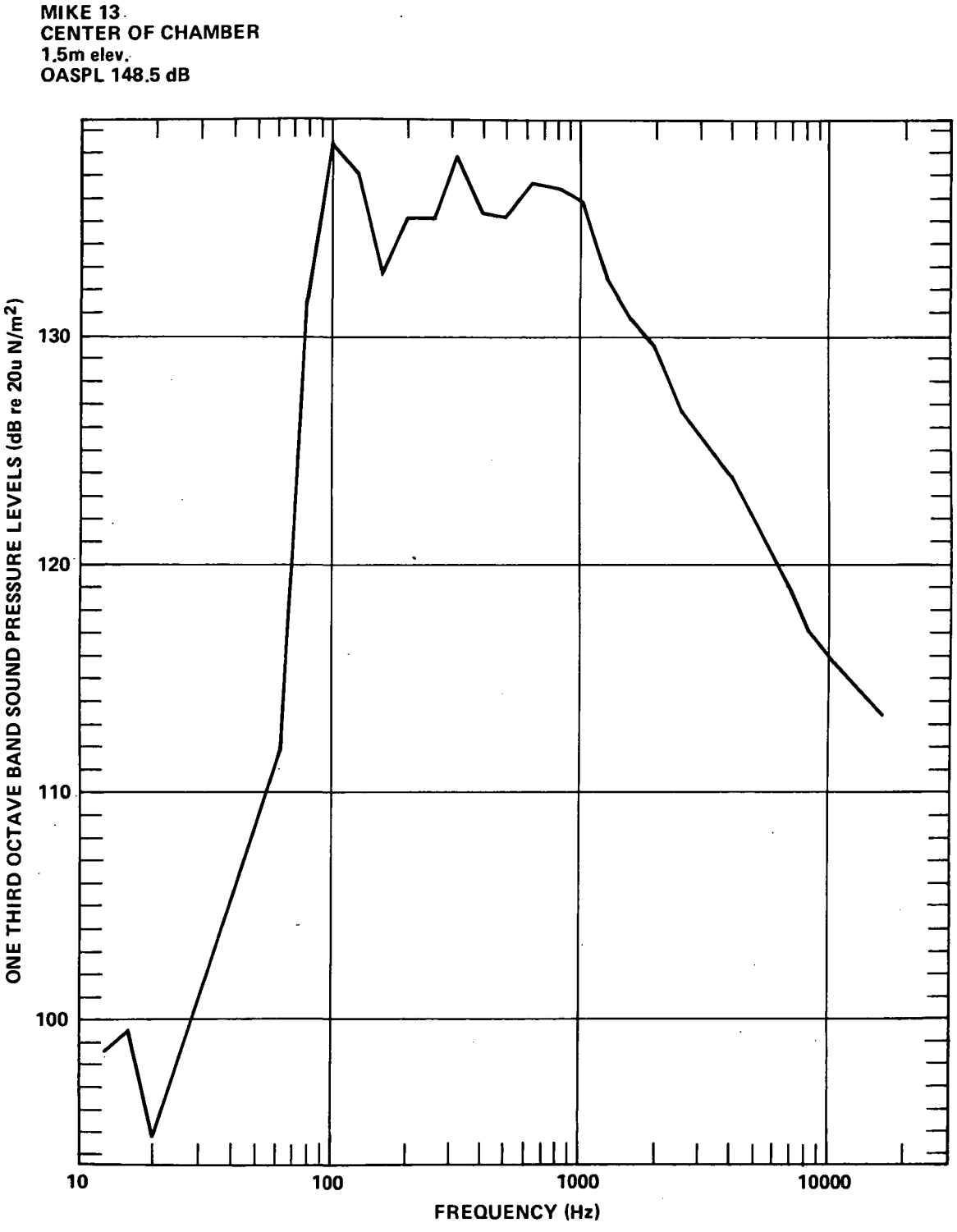

Figure 14. One-third Octave-band Analysis - Typical Microphone Channel

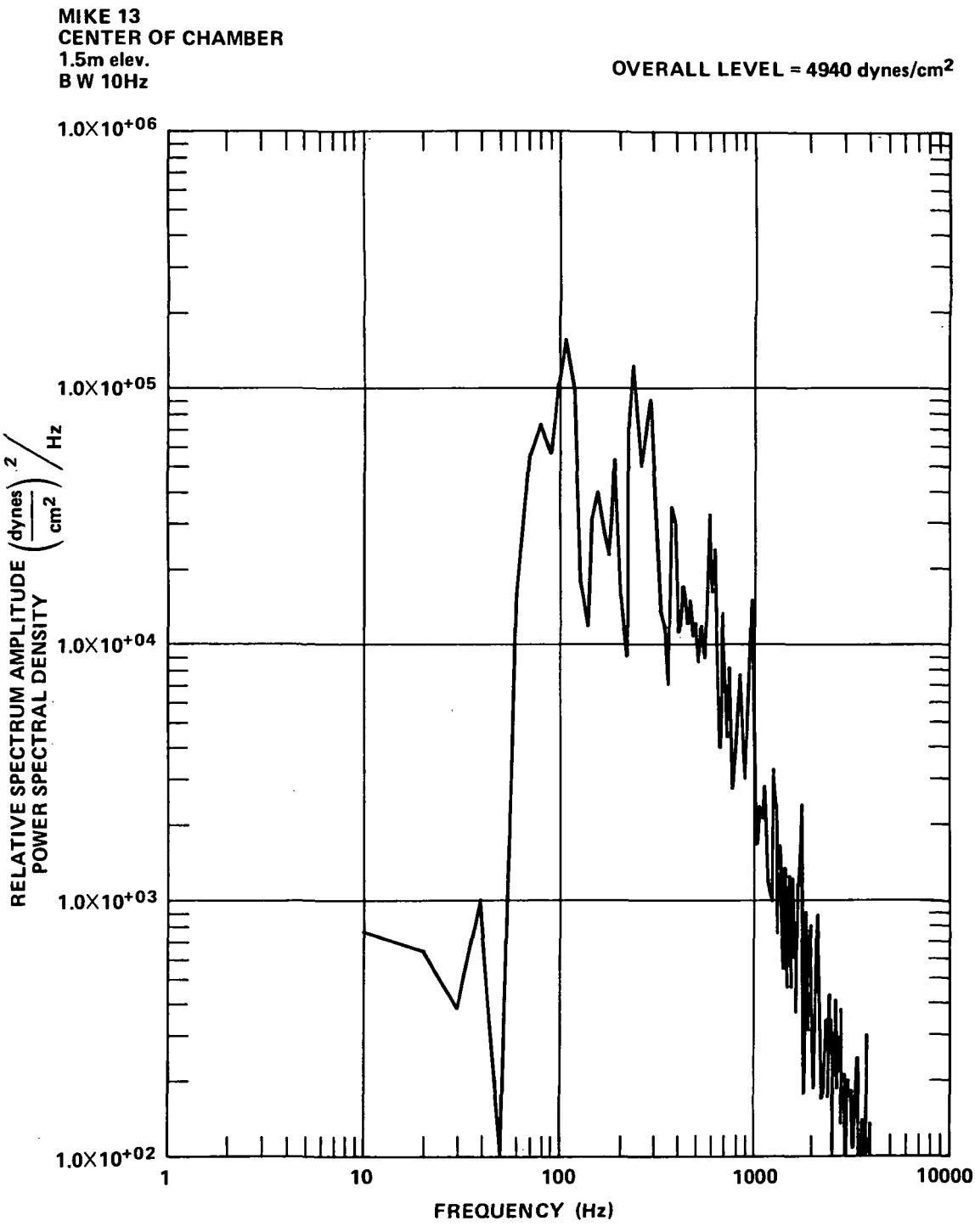

Figure 15. Power-spectral-density Analysis - Typical Microphone Channel

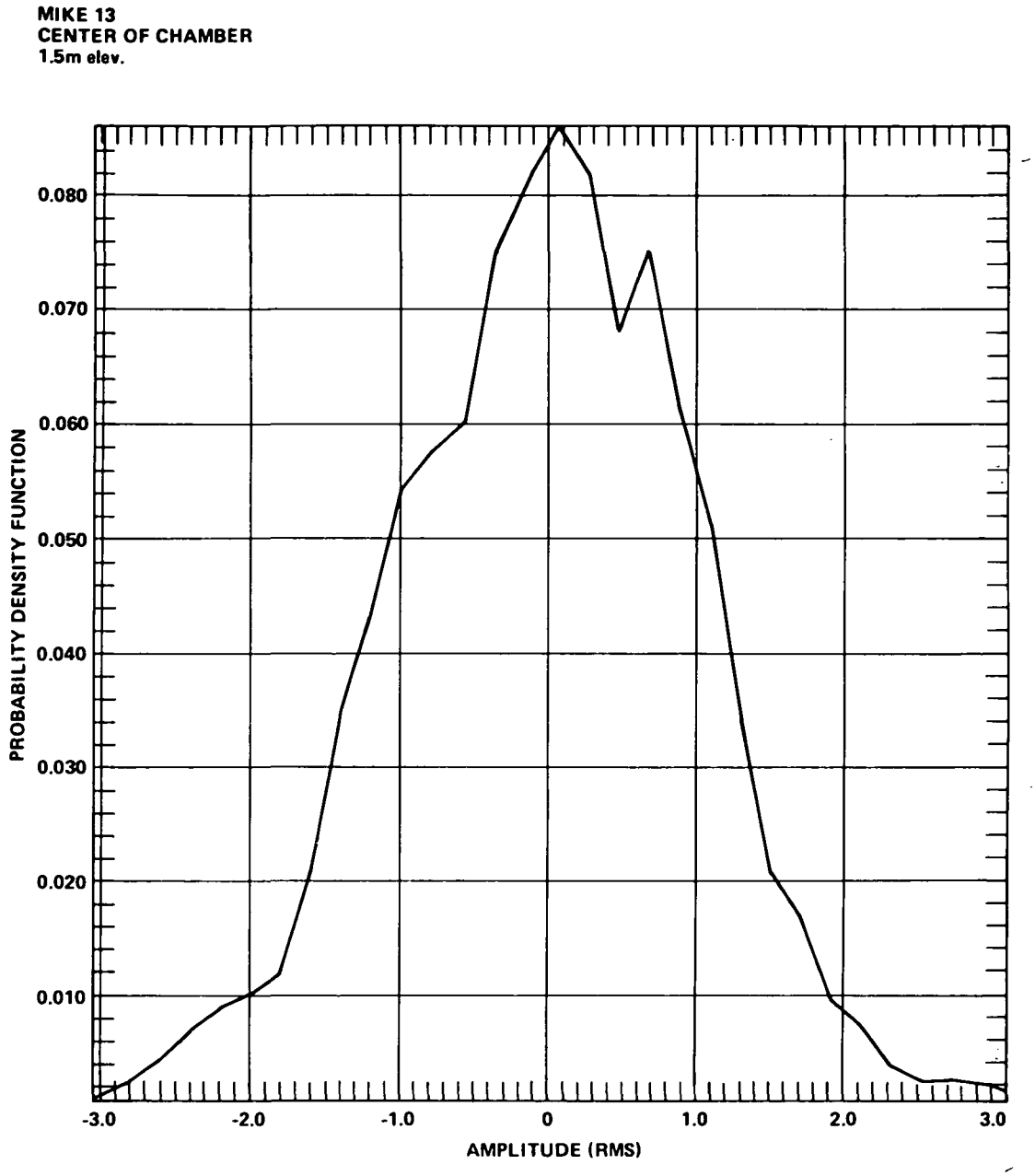

Figure 16. Probability-density Function - Typical Channel

The spatial variation data were analyzed using the Goddard DYVAN computer program. Microphones 1 through 6, and 13 (figure 5) were analyzed using a time sample of data 0.5 second and a data cutoff frequency of 12.5 kHz. Microphones 7 through 12 were analyzed using a time sample of 2.0 seconds and a data cutoff frequency of 2.5 kHz. The sample time was increased for the latter microphones, to verify that the amplitude

variations seen in the lower one-third octave bands were indeed due to the characteristics of the chamber and not due to insufficient time averaging.

The spatial variation data presented in figure 13 indicate a deviation of approximately 0.5 dB between predicted and measured values at frequencies above 500 Hz corresponding to modal overlap indices greater than 1.8. Measured values of spatial variation exceed 1.5 dB at frequencies below 350 Hz.

It is interesting to note that in figure 6 the measured reverberation times below 350 Hz exhibit irregularities of various kinds, such as double slopes and fluctuations in the mean reverberation time from frequency band to band. At frequencies above 350 Hz the decay curves show single slopes and a systematic trend in the mean slope from frequency band to band. The significance of the relationship between increasing spatial variation and erratic reverberation times will be discussed below.

The spatial variation for the occupied chamber yielded the same general shape as the empty chamber results. The noted irregularities were probably due to the boundary effects of the walls and of the test specimen. In general the frequency below which the measured values of spatial variation exceed any particular allowable maximum is seen to shift upward, relative to the frequency for the empty chamber condition, less than one octave.

Statistical Independence of Spatial Variation Data

The worst-case coherence results, indicating the approximate degree of statistical independence between the outputs of microphones located at various points on the microphone array, were shown in figure 3a. As a reference point, microphone 2 was correlated with itself and produced the expected unity coherence. As a second reference point, one microphone channel (microphone 7) was correlated with white noise of the same bandwidth (2.5 kHz) and plotted as a baseline. This baseline data served as a measure of the resoultion, as limited by the dymanic range, of the DYVAN computer program. Figure 3b, the smoothed version of figure 3a, includes the results of the coherence analysis from the Helios test.

Discrepancies below values of $2\pi fr/c = 6$, shown in figure 3a and 3b, between the measured and the theoretical predictions occurred because the theoretical predictions assume narrowband conditions (see section on microphone locations), whereas the measured variations were based on a one-third octave-band analysis procedure. Above $2\pi fr/c = 6$, the measured values are within the noise band representing the lower limit of the computer program. Since these measurements were taken independently for each of the microphone arrays (inboard or outboard) and for each elevation, the coherence between outputs of microphones located on the different radii and different elevations would be zero in theory and thus are not presented.

The spatial variation data for the occupied chamber was calculated from the seven exterior microphones ($n = 7$) used for control and monitoring during the Helios test. The statistical

independence of those microphones at these locations was also illustrated in figure 3b. As noted previously, some of these microphones were located within inches of the spacecraft skin, and thus were subject to some boundary effects.

Lowest Usable Frequency (f_c)

The lowest usable frequency for a reverberation chamber (not to be confused with horn-coupling cutoff frequency) is that frequency below which the sound field in the reverberation room ceases to have an acceptable level of spatial variation and diffuseness. This frequency may be affected by the size of the test specimen occupying the chamber.

The criteria for maximum spatial variation on a one-third octave-band basis is that the lowest one-third band showing no more than ±3-dB spatial variations and no less than one-third modal overlap index shall be specified as the lowest acceptable test frequency. Based on this criteria, the data presented in figure 13 indicate that the chamber is useful at frequencies above 160 Hz for test volumes that are less than 10 percent of the chamber volume.

The lowest usable frequency of the chamber when occupied by a test specimen of about 20 percent of the chamber volume cannot be established via the criteria on modal overlap index; the index cannot be determined without the use of reverberation times. When an equivalent criteria based on modal density considerations was employed with the criteria on spatial variation, the lowest usable frequency for a 20-percent volume specimen occupied chamber increased to 260 Hz.

In terms of the modal overlap index (M), known volume (V, in cubic meters), and the reverberation time (T_{60}, in seconds) for the mode in question, the lowest usable frequency may also be computed by

$$f_c = \left[\frac{M\, c^3\, T_{60}}{8.8\pi V}\right]^{1/2} \tag{10}$$

The value for M corresponds to the minimum value of modal overlap index ($1/3 \leqslant M \leqslant 3$), selected on the basis of an acceptable level of spatial variations of sound pressure levels within the chamber. Recall that M was based on the chamber resonant bandwidth. Equation (10) can be derived using the first term of equation (5) in (7).

The underlying logic for establishing the above criteria on the basis of a modal density or modal overlap requirement is as follows: For qualification testing or design evaluation, it is frequently desirable to express the lowest usable frequency in terms of the number of modes required within the resonant bandwidth of a structure. The required modal density can be directly related to the anticipated resonant amplification factor, Q, of the test specimen and the average number of modes desired within the specimen's resonant band, to give the proper response simulation by the following relationship:

$$n(f)\,\Delta f_r \cong \frac{4\pi V f_0^{\,3}}{c^3 Q} \geqslant \text{minimum desired or specified number of modes} \qquad (11)$$

where $\Delta f_r = f_0/Q$;

F_0 = fundamental structural mode frequency; and

Q = resonant amplification factor.

For example, if the number of modes required within a resonant bandwidth of a structure is established, and if the minimum number of modes required for proper testing is seven, then the minimum structural resonant frequency, f_0, which can be excited satisfactorily can be determined. Using the following values in equation (11),

$V = 68\ m^3$;

$c = 344$ m/s; and

$Q = 10$ (expected maximum value).

f_0 is calculated to be 150 Hz. For a resonant frequency of 150 Hz and an expected Q of 10, there is a resonant bandwidth of 15 Hz within which a minimum of seven chamber resonant modes are required. Entering the graph, figure 12, at 150 Hz, one can expect to have at least 0.7 mode at this frequency. Multiplying the number of chamber modes (0.7), times the structural resonant bandwidth (15 Hz), yields 10.5 modes in the lowest frequency band of interest (Δf_r). Note that if this criteria is fulfilled at 150 Hz, it will be exceeded, on the average, above 150 Hz, since the modal density increases with frequency. Therefore, it appears reasonable to define a lower-band frequency for a reverberant room as the lowest frequency at which the room has the required modal density, provided the spatial variation requirement is not exceeded.

Spectra-shaping Capability

The purpose of these tests was to obtain a family of curves which represent the overall levels and the spectrum-shaping capabilities of the reverberation chamber/generator system. The data points on these curves are the spatial average of pressure levels obtained from three microphones located at elevations of 1.52 m, 3.04 m, and 4.12 m at the center of the empty chamber. For the occupied chamber data the microphones were located as shown in figure 4b.

Shaping Capability at Intermediate Sound Pressure Levels

The bulk of the aerospace acoustic testing done at Goddard requires overall sound pressure levels (OASPL) on the order of 145 to 153 dB. The sound pressure levels are achieved in the Goddard chamber by use of the Noraircoustic generator, which employs a hydraulic exciter driven by a rather narrowband (700 Hz) of random noise to modulate the airstream.

The full frequency range output is achieved through the generation of random harmonic bands which fill in above the fundamental random input band. By achieving a balance between air stream power and exciter power, a flat output spectrum is obtained. Below the maximum output, emphasis of the high- or low-frequency portions of the spectrum (450-Hz crossover) can be accomplished by shifting the balance between airstream power and exciter power.

By utilizing the above principles of operation, three curves representing the overall shaping capability were plotted on an octave-band basis, and these are shown in figure 17. For the flat spectrum output and the emphasized high-frequency and low-frequency spectrum curves, the corresponding control parameter (air and/or signal drive level) was varied to determine over what dynamic range of sound pressure level the same approximate shape can be maintained. For comparison purposes the maximum output capability of the facility is also shown.

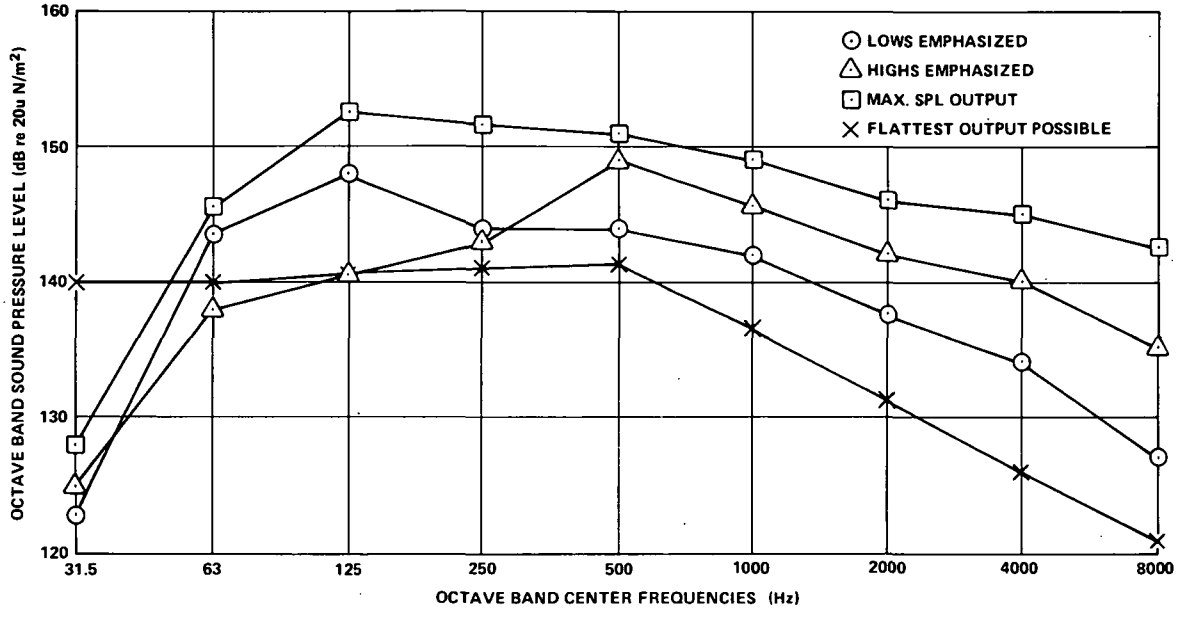

Figure 17. Spectrum Control - Reverberant Chamber

These curves give an idea of the overall shaping capability available. The curves were taken with no derating orifice installed in the noise generator. Previous studies showed that a dynamic range of about 6 dB is available, over which the above input parameters can be varied and the generator output correspondingly raised or lowered while maintaining the same spectral shape. With derating orifices, a total range of 20 dB is available from approximately 135-dB to 155-dB overall sound-pressure level.

It should be noted that, for this noise source or any other noise source, the maximum overall output is dependent on the degree of shaping (spectral distribution of energy) required. For the Mark V noise source, the overall sound pressure level drops from 5 to 10 dB below maximum output as shown in figure 17.

Effects of Test Volume Size on the Reverberant Noise Field

One of the most important requirements to be satisfied by the designer of a reverberation chamber is to provide a generator/chamber configuration capable of reproducing a given noise spectra. The reproducibility of noise spectra, within the GSFC chamber, for three commonly used launch vehicles (Atlas Centaur, Improved Delta, and Titan III-C) and for the acoustic noise portion of DOD Military Standard 810B was assessed under empty chamber conditions. In all cases the noise spectra was reproducible within ±3 dB.

When testing the Helios spacecraft to the Titan III-C acoustic requirements, insignificant differences were observed between the four-channel average of the empty chamber spectrum and the spectrum obtained with the Helios in the chamber. On the basis of these results a test specimen volume of 20 percent of the chamber volume should have a negligible effect on the spectral shape as normally measured during acoustic tests. Wyle Laboratories has done some model study work in this area which supports this tentative conclusion (reference 8).

Figure 18 is a plot taken from the Wyle study. These data were taken from a very small scaled model with room dimension ratios of 1:0.82:0.71. The plot shows the sound-pressure levels measured in the chamber with various specimen sizes relative to sound-pressure levels measured in the empty room. The fact that the curves for the 9-percent and 25-percent volumes are displaced from the zero difference line may be due to the size of the scale model chamber that was used. Superimposed on this plot are similar results from the Helios Test.

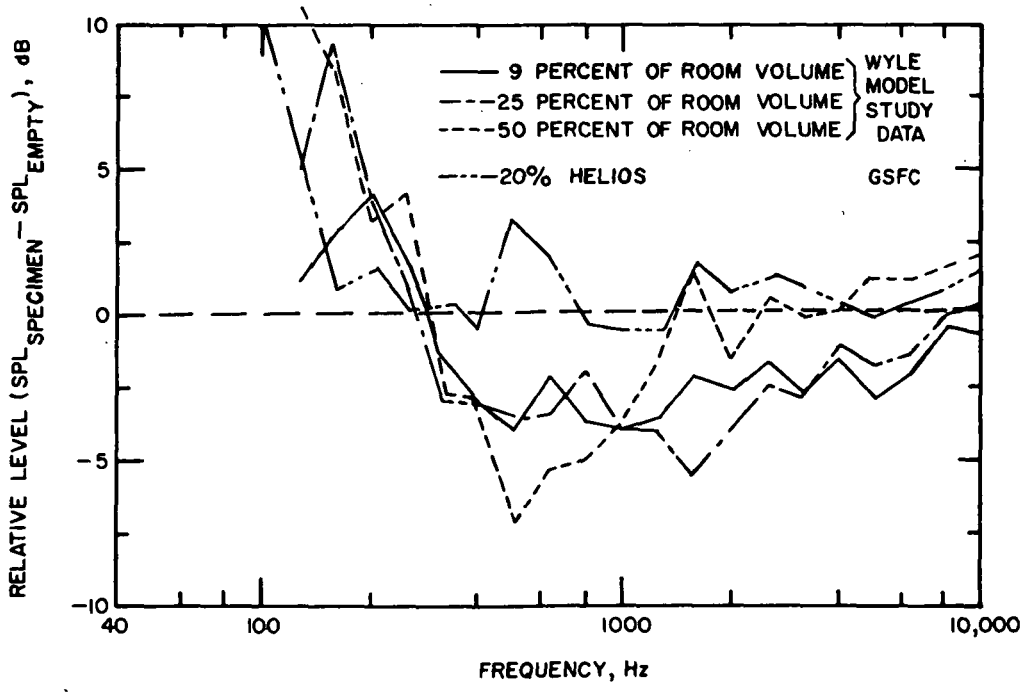

Figure 18. Sound-Pressure Levels Measured in a Reverberation Room with Various Specimen Sizes Relative to Sound-Pressure Levels Measured in the Empty Room

The results from the GSFC chamber are more promising than what was expected, as indicated by the scale model data. The increasing difference in SPL between the occupied and empty chamber results, with increasing specimen size, at the low frequency end of the spectrum is due primarily to reduction in chamber volume caused by the specimen. During the model study, an extended frequency scale was used to collect sine sweep test data. The data indicate that the longer average path lengths followed by the sound rays in passing around the specimen result in a general lowering of the individual resonances of the chamber. This lowering of the resonances has the effect of spreading the peaks out in the lower frequency range, so that the chamber is even less usable at these low frequencies than when it is empty. This spreading of peaks was also demonstrated by the increase of spatial variation in figure 13.

Based on these results, the GSFC chamber occupied by a specimen having a volume of 20 percent of the chamber volume would not be considered to seriously degrade the chamber performance. Moreover, for specimens having sufficiently low resonant magnification factors, a specimen as large as 50 percent of chamber volume possibly could be tested.

Maximum Achievable Sound-Pressure Level And Spectral Noise Distribution

The calculation of the sound power delivered to a reverberant room is a rather involved process. Two slightly different approaches are taken in this section. The first approach predicts the sound-pressure level (SPL) delivered to the room on an overall sound-pressure level basis using the nominal rated generator power output of 50,000 watts into a progressive wave chamber. This prediction was adjusted downward by 6 dB, an amount empirically determined by Mills (reference 9), and later described by an analytical expression (reference 10). The predicted and measured values agreed at the mouth of the horn. The additional 4.5- to 5.5-dB difference between the measured and predicted values was attributed to horn extension losses.

In the second approach, a one-third octave-band plot (obtained from the manufacturer) of the generator power output, using a white noise input, was converted to one-third octave-band sound-pressure levels. The measured sound-pressure level in the chamber using the same white noise input was then compared to the converted manufacturer's data. The results were in good agreement when the different operating conditions were taken into consideration.

Determination of the Maximum Overall Sound-pressure Level (OASPL)

The maximum, overall, space-averaged sound-pressure level in the reverberation chamber was predicted from the following classical equation that relates maximum sound power level (PWL_M) delivered to a reverberant room, the room volume, and the reverberation time:

$$SPL_M = PWL_M - 10\log_{10} V + 10\log T_{60} + 4.0 \quad (12)$$
(Reverb.)

where SPL is in dB referenced to 20×10^{-6} N/m^2;

PWL = 171 dB and referenced to 10^{-13} watts;

V = 68 m^3; and

T_{60} = 6 seconds (average value 50 - 2 kHz).

The PWL value was obtained by using the rated generator output (50,000 watts-progressive wave, PWL = 177 dB), and an overall minus 6 dB correction, computed using equation (13).

It has been noted that when the overall sound-power level in equation (12) is evaluated on the basis of measurements of sound power delivered by an acoustic driver into a progressive wave chamber, equation (12) yields a prediction in OASPL which is approximately 6 dB higher than that measured by Mills (reference 9). For this reason, at least one manufacturer of acoustic drivers has recommended a modification of equation (12). The numerical factor on the right hand side is replaced by -2.0 when PWL is obtained from progressive wave chamber data.

This apparent discrepancy between equation (12) when using progressive wave data and the results based on actual measurements appears to be due to two possibilities: The first possibility is that the classical relationship between sound-pressure level in a diffuse reverberant field and source-power level, as in equation (12), assumes that the modal density in the room approaches infinity for all frequencies, such that all power delivered to the room is uniformly amplified. Clearly this is not the case at low frequencies where individual resonant modes are widely spaced. As a consequence of the gaps between the modes, only that power which is within the frequency range of the mode is amplified; all other power is lost. The second possible reason for the discrepancy is that the output characteristics of an electropneumatic transducer, when driving a resonant system, are not well understood. There is a possibility of a change in the impedance loading on the transducer/horn system with a corresponding change in output power.

Recent analyses (reference 10) support the first possible cause and accounts for the noted discrepancy between the classical prediction given by equation (12) and the prediction by Mills' equation (reference 9). In reference 10, the sound-power level delivered to a reverberant room in terms of the sound power delivered to a progressive wave chamber by the same high intensity acoustic source (acoustic driver plus coupling horn) is given by the following expression:

$$(PWL_M)_{\substack{\text{Reverberation}\\\text{Room}}} = (PWL_M)_{\substack{\text{Progressive}\\\text{Wave Chamber}}} - 10\log\left(\frac{M+1}{M}\right) \quad (13)$$

where M is an appropriate modal overlap index of the reverberation room. Substituting this relationship in equation (12) will permit prediction of the reverberant chamber levels using sound power levels measured in a progressive wave chamber.

Equation (13) indicates that at high frequencies where the modal overlap $M > 1$, the power delivered by the driver to the reverberant room will be equal to the power delivered to the progressive wave chamber. However, at lower frequencies where $M < 1$, equation (13) indicates that the power delivered to a reverberant room will fall off 6 dB per octave as frequency is decreased with respect to that delivered to a progressive wave chamber, assuming reverberation time is constant with frequency. This analytical result expressed in equation (13) is compatible with experimental data (reference 9).

The maximum overall sound-pressure level was measured using both the Noraircoustic Mark V and the Ling EPT-94B generators. As shown on figure 17, for maximum sound-pressure level of the Mark V on an octave-band basis, the spectrum is fairly flat out to 700 Hz, with a 2.5 dB per octave rolloff above 700 Hz. Table 5 gives the predicted overall sound-pressure level using equation (12) and the predicted value using the empirical correction developed by Mills. The measured value in the reverberant area of the chamber using the Mark V is seen to be 158.5 dB overall, whereas the value predicted by Mills (164 dB) occurs at the horn mouth (163 dB).

Table 5

Summary of Measured and Predicted Overall Sound Pressure Levels for Reverberation Room Using a Shaped White Noise Input

Generator	Predicted Equation 12 (Classical)	Predicted (Empirical Correction to Equation 12)	Measured Center of Chamber 1.5 m Elevation	Measured Horn Mouth
Noraircoustic Mark V	170.47	164.02	158.5	163
Ling EPT-94B	160.0	154.0	148.0	154

The additional decrease of 4.5 to 5.5 dB between the value predicted by Mills' equation and that measured in the reverberant field was anticipated and is the result of a design tradeoff between maximum chamber volume, optimum horn coupling to the room, and practical considerations in locating the room. It was believed that the additional volume

with its lower cutoff frequency and larger usable floor plan was of more value as long as the available sound-pressure level was adequate for all foreseeable test requirements. This compromise was effected by considering the north and south oblique walls and floor as straight line extensions of the tangent to the horn surface at the end of the horn. However, it was also anticipated that these extensions might increase the radiation resistance seen by the source/horn system, and hence increase the radiated power to the room by as much as 3 dB. The increase in radiated power was offset by losses along the increased effective length of the horn. Data indicate that the reverberant field was fully developed beyond a distance of one meter from the mouth of the horn.

An alternative approach to the room design, using the same limited space, would have been a rectangular room of less than half the volume. The horn would then have been coupled into the room at a corner with approximately the same increase in radiation resistance. The reverberant field would be developed closer to the horn with approximately a 2- to 3-dB increase in overall sound-pressure level.

Determination of Chamber Spectral Noise Distribution

The predicted and measured one-third octave-band sound-pressure level distribution for the reverberation chamber for a white noise input (63 to 1,000 Hz), are compared in figure 19. The predicted results were obtained via the use of equation (10), which was modified to reflect the frequency dependency of the modal density and the reverberation time of the chamber. Equation (12) can be rewritten as:

$$1/3\ \mathrm{OBSPL}_{\mathrm{Reverb}} = 1/3\ \mathrm{OBPWL}_{\mathrm{Prog}} - 10 \log \frac{M(f)+i}{M(f)} + 10 \log T_{60}(f) - 10 \log V + 4.0 \qquad (14)$$

where V is in cubic meters.

Manufacturer's data for the Mark V generator were used. These data were taken with the Mark V driving a 50-Hz horn terminated in a free-field, white noise input. The microphone was located at a point 1.82 meters downstream from the exit orifice of the generator. Data were presented as sound-power level versus one-third octave-band center frequency.

The predicted and measured overall values for white noise inputs, shown in figure 19, while similar in shape, differ in overall level by 11 dB. This difference is due primarily to the different operating conditions under which the measurements were taken, and can be accounted for as follows: The efficiency of the Noraircoustic generator was determined by the manufacturer by measuring the acoustic power in a 50-Hz horn at a point 1.82 meters downstream of the generator exit orifice. Horns with different cutoff frequencies and lengths require modification of the rated power to obtain the delivered power. To obtain the delivered power to the chamber under study, two losses must be considered: (1) the horn factor (0.5 dB for 60 Hz, in reference to 50-Hz cutoff) and (2) the path length loss gradient. The path length extends from a point 1.82 meters downstream of the generator to a point one meter out into the room (a total of 2.20 meters) and has a measured loss gradient of approximately 5 dB per meter or a total loss of

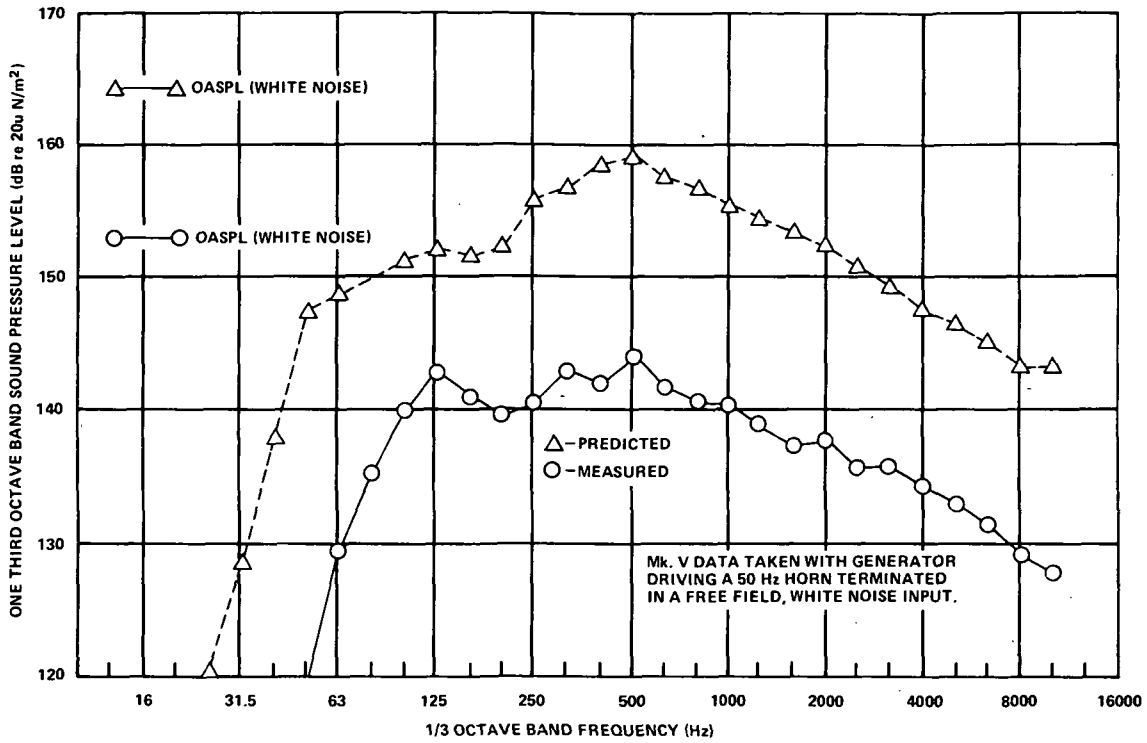

Figure 19. Predicted Versus Measured One-third Octave-band Sound Pressure Level Distribution in Reverberation Chamber Using Noraircoustic Mark V Acoustic Generator

11.0 dB. If the power losses are accurately calculated on an overall sound-pressure-level basis, equation (14) can be of value in predicting the spectral shape for a particular chamber configuration.

CONCLUSIONS

The investigation to obtain experimental data with which to verify the predicted performance of the GSFC truncated reverberation chamber and to assess the effect of various sized test specimen volumes on chamber performance resulted in the following conclusions:

1. The extremely close correlation obtained between predicted data, model study data, and measured data permit using existing theory to predict the chamber noise field and test item response with a high degree of confidence.

2. Test specimen volumes of up to 20 percent of the chamber volume are shown to have a negligible effect on the acoustic noise field when measured on an averaged one-third octave basis. A closer examination on a narrowband statistical basis reveals only small changes which, when understood by the test engineer, provide a basis for justifying the testing of even larger test specimen volumes, up to 50 percent of the chamber volume.

3. A simplified method of measuring reverberation time, using broadband rather than the conventional narrowband noise excitation, yields for all practical purposes results which are identical to those obtained with the narrowband excitation.

4. All frequencies now specified or anticipated in acoustic test specifications can be reproduced satisfactorily. The lowest usable frequency, assuming a maximum allowable spatial variation of ±3.0 dB, is 160 Hz. For many tests, the chamber is adequate below this frequency. Data are presented for determining the degree of compromise necessary in chamber performance for operation at lower frequencies.

5. Maximum versatility in spectra shaping is obtained by using two air modulators. While the bulk of this evaluation was performed using the Noraircoustic Mark V generator, a limited amount of the evaluation was performed using the lower-powered Ling EPT-94B as a noise source. From extensive previous experience with the Ling source, the authors feel that the Ling generator will provide superior shaping capability (at lower overall levels, 148 dB maximum) on a one-third octave-band basis over the range of 100 to 1,000 Hz.

Goddard Space Flight Center
National Aeronautics and Space Administration
Greenbelt, Maryland May 1974
502-22-11-01-51

REFERENCES

1. Sepmeyer, L. W., "Computer Frequency and Angular Distribution of the Normal Modes of Vibration in Rectangular Rooms," *J. Acoust. Soc. Am.*, 37, 3, 1965.

2. Scharton, T. D., P. E. Rentz, D. Lubman, and P. H. White, *Techniques for Improving the Low Frequency Performance of Small Reverberation Chambers,* NASA NAS5-21003, NAS CR-112407, Bolt, Beranek and Newman, Inc., California, 1970.

3. Beranek, L. L., *Acoustics,* McGraw-Hill Book Company, Inc., New York, 1954.

4. Morse, P. M., and K. U. Ingard, *Theoretical Acoustics,* McGraw-Hill Book Company, Inc., New York, 1968, p. 597.

5. Beranek, L. L., *Noise Reduction,* McGraw-Hill Book Company, Inc., New York, 1948, p. 235.

6. Morse, P. M., *Vibration and Sound,* McGraw-Hill Book Company, Inc., New York, 1948, section 32.

7. Bolt, R. H., and P. W. Roop, "Frequency Response Fluctuations in Rooms," *J. Acoust. Soc. Am.*, 22, 2, 1956.

8. Cockburn, J. A., *Evaluation of Acoustic Testing Techniques for Spacecraft Systems,* NASA NAS5-21203, NAS CR-122450, Wyle Laboratories, Alabama, 1971.

9. Mills, J. F., "A Study of Reverberation Chamber Characteristics," *1967 Proceedings of the Institute of Environmental Sciences, 13th Annual Technical Meeting,* 1967, figure 10.

10. Scharton, T. D., and P. H. Smith, "The Average Resistance and Conductance of Vibratory and Acoustic Systems," *J. Acoust. Soc. Am.*, to be published.

APPENDIX

GENERAL PERFORMANCE DATA FOR THE 68-CUBIC METER REVERBERANT NOISE CHAMBER, GODDARD SPACE FLIGHT CENTER

GENERAL PERFORMANCE DATA, EMPTY CELL

Maximum Overall Sound Pressure Level,	
Noraircoustic Generator Mark V -	158.5 dB*
Ling EPT-94B -	148 dB

SPECTRUM SHAPING CAPABILITY

Output flat from 100 to 700 Hz, ±1.5 dB.

Low-frequency rolloff, 125 to 63 Hz -	6 dB/octave
63 to 31.5 Hz -	18 dB/octave
High-frequency rolloff,	
Minimum rate, 500 Hz to 10 kHz,	3.5 dB/octave
Maximum rate, 500 Hz to 4 kHz,	5 dB/octave
4 to 10 kHz,	8 dB/octave
Dynamic Range (Overall sound pressure level) over which the spectrum shape can be held constant -	20 dB (135 to 155 dB)

CHAMBER NOISE-FIELD CHARACTERISTICS

Spatial Variation -
Less than ±1.5 dB above 350 Hz, Modal Overlap, 1.00
Less than ±2.5 dB above 180 Hz, Modal Overlap, 0.3
Less than ±3.0 dB above 160 Hz, Modal Overlap, 0.25

Modal Density -
At least seven modes per one-third octave band starting at 80 Hz.

Average Reverberation Time - 50 Hz to 2 kHz - (With air at 297°K, 24°C, R.H. 55%)	6 seconds
Average Absorption Coefficient -	1.5%
Horn Cutoff Frequency -	60 Hz
Propagating Medium -	Gaseous Nitrogen

*All dB notations are referenced to 20×10^{-6} N/m^2..

DATA COLLECTION AND ANALYSIS

Instrumentation -

Bruel and Kjaer or Altec Microphones	15 channels
Crystal Microphones or Accelerometers	42 channels
Bridge-type Transducers, Strain gages and others	18 channels

Closed-circuit Television, Monitor, and Video Recorder.

Miscellaneous Cabling, 32 conductors

Data Analysis -

Real time, 1/1, 1/3 octave band.
Offline, 1/1, 1/3, 1/6, 1/10, and narrowband.

CHAMBER FACILITIES

AC Power -	115 VAC, 20A; 208V, 3ϕ, 20A
Hydraulic Pressure -	20.682×10^6 N/m^2 (3,000 psi) 1.26×10^{-3} m^3/sec (20 gpm)
Compressed Air -	6.894×10^5 N/m^2 (100 psi)
Hoist -	1,812 kg (4,000 lb) 10.2 cm/min (4 inches/min)

Note. Spectrum control and monitoring is accomplished with a General Radio, model 1921, one-third octave-band realtime equalizer/analyzer system. Microphone averaging of up to six control points is available. The use of multichannel averaging control insures that the control sound-pressure level will approach the average SPL over the test volume; that is, the control SPL is centered within the inherent spatial variation of the chamber.

NATIONAL AERONAUTICS AND SPACE ADMINISTRATION
WASHINGTON, D.C. 20546

OFFICIAL BUSINESS
PENALTY FOR PRIVATE USE $300

SPECIAL FOURTH-CLASS RATE
BOOK

POSTAGE AND FEES PAID
NATIONAL AERONAUTICS AND
SPACE ADMINISTRATION
451

U.S.MAIL

"The aeronautical and space activities of the United States shall be conducted so as to contribute . . . to the expansion of human knowledge of phenomena in the atmosphere and space. The Administration shall provide for the widest practicable and appropriate dissemination of information concerning its activities and the results thereof."

—NATIONAL AERONAUTICS AND SPACE ACT OF 1958

NASA SCIENTIFIC AND TECHNICAL PUBLICATIONS

TECHNICAL REPORTS: Scientific and technical information considered important, complete, and a lasting contribution to existing knowledge.

TECHNICAL NOTES: Information less broad in scope but nevertheless of importance as a contribution to existing knowledge.

TECHNICAL MEMORANDUMS: Information receiving limited distribution because of preliminary data, security classification, or other reasons. Also includes conference proceedings with either limited or unlimited distribution.

CONTRACTOR REPORTS: Scientific and technical information generated under a NASA contract or grant and considered an important contribution to existing knowledge.

TECHNICAL TRANSLATIONS: Information published in a foreign language considered to merit NASA distribution in English.

SPECIAL PUBLICATIONS: Information derived from or of value to NASA activities. Publications include final reports of major projects, monographs, data compilations, handbooks, sourcebooks, and special bibliographies.

TECHNOLOGY UTILIZATION PUBLICATIONS: Information on technology used by NASA that may be of particular interest in commercial and other non-aerospace applications. Publications include Tech Briefs, Technology Utilization Reports and Technology Surveys.

Details on the availability of these publications may be obtained from:

SCIENTIFIC AND TECHNICAL INFORMATION OFFICE

NATIONAL AERONAUTICS AND SPACE ADMINISTRATION

Washington, D.C. 20546